ADVANCED MATERIALS
www.advmat.de

Living Matter: Mesoscopic Active Materials

Anne Bernheim-Groswasser, Nir S. Gov, Samuel A. Safran, and Shelly Tzlil*

An introduction to the physical properties of living active matter at the mesoscopic scale (tens of nanometers to micrometers) and their unique features compared with "dead," nonactive matter is presented. This field of research is increasingly denoted as "biological physics" where physics includes chemical physics, soft matter physics, hydrodynamics, mechanics, and the related engineering sciences. The focus is on the emergent properties of these systems and their collective behavior, which results in active self-organization and how they relate to cellular-level biological function. These include locomotion (cell motility and migration) forces that give rise to cell division, the growth and form of cellular assemblies in development, the beating of heart cells, and the effects of mechanical perturbations such as shear flow (in the bloodstream) or adhesion to other cells or tissues. An introduction to the fundamental concepts and theory with selected experimental examples related to the authors' own research is presented, including red-blood-cell membrane fluctuations, motion of the nucleus within an egg cell, self-contracting acto-myosin gels, and structure and beating of heart cells (cardiomyocytes), including how they can be driven by an oscillating, mechanical probe.

1. Introduction

Herein, materials scientists are presented with an introduction to the physical properties of living active matter at the mesoscopic scale (tens of nanometers to micrometers) and their unique features compared with "dead," nonactive matter. This field of research is increasingly denoted as "biological physics"[1] where physics includes chemical physics, soft matter physics,[2] hydrodynamics, mechanics, and the related engineering sciences. The focus is usually on the emergent properties of these systems and their collective behavior which results in active self-organization[3] and how they relate to cellular-level biological functions. These include locomotion (cell motility and migration) forces that also give rise to cell division, the growth and form of cellular assemblies in development, the beating of heart cells, and the effects of mechanical perturbations such as shear flow (in the bloodstream) or adhesion to other cells or tissues. The insight gained in the study of natural biological systems also facilitates the design, fabrication, and control of in vitro biomimetic systems such as engineered tissues, "printed" organs, and microrobotics. While the mesoscale behavior of biological cells is relevant to large length scales and long time scales—compared with molecular sizes and binding/unbinding times—they are a direct result of the unique properties of the protein molecules found in these systems, such as energy consuming/releasing monomers that assemble/disassemble into polymeric structures or energy consuming molecular motors. Other applications of the physical sciences to biology, such as those aspects of biophysics that focus on the characterization of biomolecules and cells at the molecular level using physical tools, or systems biology that is concerned with top-down descriptions of large chemical or neuron networks, do not focus on the macromolecular interactions, forces, and collective motions that are the center of attention of biological physics.

Many—but certainly not all—advances in applying physical measurements and concepts to observed phenomena are made by examining relatively large-scale or long-time phenomenon and studying the behavior as a function of physically controlled parameters (as opposed to chemical modifications). This has a long history in diverse systems in materials science such as superconductivity (Ginzburg–Landau ideas and experiments on vortices), polymers (scaling concepts and measurements by the de Gennes "school"), phase transformation dynamics (pioneering approach of John Cahn and scattering experiments of spinodal decomposition), and the mesoscale properties of elastic inclusions (as formulated by Eshelby). These approaches "coarse grain" many of the molecular details of the system that allows the behavior to be described using a minimal theory that lumps the molecular details in a very small number of parameters. The focus of the theory is to predict behavior as a function of physical inputs that can be experimentally controlled to give different types of qualitative behavior. The molecular components are of course critical, but often times only modify the effective parameters at the small scale: for example, the persistence length of a polymer sensitively depends on its chemistry, while scattering measurements of the radius of gyration

Prof. A. Bernheim-Groswasser
Department of Chemical Engineering and Ilse Katz Institute for Nanoscale Science and Technology
Ben Gurion University of the Negev
Beer-Sheva 84105, Israel
Prof. N. S. Gov, Prof. S. A. Safran
Department of Chemical and Biological Physics
Weizmann Institute of Science
Rehovot 7610001, Israel
E-mail: sam.safran@weizmann.ac.il
Dr. S. Tzlil
Department of Mechanical Engineering
Technion
Haifa 3200003, Israel

DOI: 10.1002/adma.201707028

 © 2018 WILEY-VCH Verlag GmbH & Co. KGaA, Weinheim

of the entire chain as a function of its overall length focus on the mesoscale behavior and scaling exponents. In the examples presented here of mesoscale properties of active biological systems, the situation is similar. The active undulations of membranes, contraction of actomyosin gels, cytoskeletal order in the cells, and the beating of cardiomyocytes discussed below are studied experimentally and theoretically at the mesoscale. The molecular involvement of unique biomolecules such as actin, myosin motor proteins, focal adhesion proteins, passive crosslinking proteins, and lipids is crucial but the generic behavior at long times and large spatial scales does not require very detailed knowledge of the short-scale properties beyond a few general features that we outline in this review.

The large-scale protein assemblies that give many cells their structural integrity and shape memory do so because of their unique self-assembling structures combined with active, nonenergy conserving, forces that can cause deterministic motion. One of the major components that determine cell structure are actin filaments comprising semiflexible, self-assembled polymers whose basic units are monomers of a globular protein named G-actin. Due to the asymmetric (i.e., polar) structure of actin monomers, an actin filament (F-actin) is also polar, with two ends having different affinity, and therefore, different binding constants for monomeric actin as well as different polymerization/depolymerization rates. This polarity is also important for molecular motor movement along actin tracks. Active forces within the cell arise from energy consumption via metabolism[4–6] and result in molecular conformations that can be very far from their ground state even if thermal fluctuations are included. Such effects are responsible for the motions involved in muscle contraction, wound healing, embryo development, cell migration, and cancer metastasis. Much of the intellectual basis for the understanding and measurement of the membranes, polymer-like muscle fibers, and wetting-like crawling of cells is found in the discipline of synthetic soft matter (e.g., membranes, polymers, and wetting droplets). However, the major challenge for the physical scientist interested in cell biology rests in coupling this knowledge with the various chemical reactions that cause biological systems to often operate far from thermal equilibrium due to the internal energy sources within the cell.

While the basic polymer structure and self-assembly of actin and the local electrostatic interactions of actin and myosin motors are related to analogous phenomena in equilibrium (nonactive) materials,[2] the unique function of acto-myosin within the cell arises from the coupling between mechanical work and chemical activity (including ATP hydrolysis and actin-myosin binding/unbinding events) that allows for the directional motions of myosin molecules along actin tracks; this eventually leads to the locomotion of the whole cell or even an entire organism.

While the examples discussed above are in the cellular context, the combination of soft matter physics—which governs the structure and macromolecular dynamics—and biochemical activity—which governs the nonequilibrium nature of important biological processes—is also important in synthetic contexts. Examples include the use of DNA attached to surfaces to form active polymer "brushes" (a well-studied subject in polymer physics and chemistry) and using polymer physics to

Anne Bernheim-Groswasser is a faculty member in the Chemical Engineering Department at Ben Gurion University. The main subject of the research of her group focuses on in vitro reconstitution of cellular processes, such as cell motility and cell shape changes, using purified proteins. This approach consists of designing model systems in which the geometry and protein composition is fully controlled. Among their main interests is the role of active contractility on pattern formation and shape transformation of actomyosin gels coupled or decoupled from membrane surfaces. They are also interested in studying cooperative effects driven by groups of motor proteins.

Nir S. Gov is a faculty member of the Department of Chemical and Biological Physics at the Weizmann Institute of Science. He develops theoretical models, using physics approaches such as statistical physics, equations of motion, and nonlinear dynamics to describe a range of biological phenomena, from active fluctuations within cells to the collective motion and decision making of animal groups. The aim is both to explain the underlying mechanisms that give rise to the observed biological phenomena and to obtain fundamental, physical understanding of new nonequilibrium systems.

Shelly Tzlil received her B.Sc. degree in chemistry and computer science (2000) and completed her Ph.D. degree in statistical mechanics of biological systems with Prof. Avinoam Ben Shaul (2006) at the Hebrew university (Israel). As a postdoctoral fellow, she joined Prof. David Tirrell's group at Caltech (USA), where she made a transition to predominantly experimental work, studying cell mechanosensing and the design of protein-engineered biomaterials. She joined the Mechanical Engineering Faculty at the Technion as a faculty member in 2012. Her current research focuses on the role and the physical mechanisms of mechanical communication between cells.

© 2018 WILEY-VCH Verlag GmbH & Co. KGaA, Weinheim

control the conditions under which DNA is actively transcribed and translated to produce proteins.[7] Other examples involve in vitro processing of stem cells in tissue engineering (e.g., artificial muscles or connective tissue) where active acto-myosin contractility plays an important role.[8]

In this review, we present an introduction to the fundamental concepts with selected examples related to our own research; a comprehensive review of the many types of biological active matter is far beyond the scope of this article. We begin in Section 2 with a discussion of the fundamental statistical–dynamic difference between thermal fluctuations and active ones. Examples are given in systems such as red-blood-cell membrane fluctuations (flickering observed under a microscope), acto-myosin-induced fluctuations in the cell interior (cytoplasm) and the directed motion of the nucleus within an egg cell. Section 3 discusses how myosin activity can promote contraction and shape transformations of thin acto-myosin gels.[9] Moreover, we show that a flow of solvent is generated during gel contraction, thereby demonstrating that the acto-myosin gels behave as poroelastic[10,11] active materials, as previously proposed for actin gels in living cells.[12,13] These results may shed light on macroscopic shape changes of 2D tissues observed in various biological systems induced by myosin contractility, for example, gastrulation in developing embryos.[14–16]

For adhered cells, acto-myosin fibers are connected at their ends, or elsewhere along their lengths, to the underlying substrate (or 3D matrix) and cannot just slide due to the myosin forces. Instead, the double-headed myosin motors end up exerting contractile forces on the oppositely polarized, actin polymers. Contractile cells also exert mechanical forces on the substrate or matrix via the adhesions that connect them. We then focus theoretically in Section 4 on the implications of contractility of many acto-myosin segments within a cell or among entire cells in gels, for the orientational[17] or translational[18–20] self-assembly of these segments or cells.[21] It is also shown theoretically how elastic interactions of such contractile units, while analogous to inclusions as studied in materials science,[22] result in very different types of acto-myosin order due to the role of activity.[21] Experimental examples are then discussed. The application of dynamical, mechanical signaling to beating heart cells (cardiomyocytes) is discussed experimentally in Section 5 where recent experiments demonstrate how an oscillating mechanical probe can "entrain" the frequency of cardiomyocyte beating. Furthermore, it is shown that the same mechanical effect can occur for two adjacent heart cells, separated by distances of several cell diameters. This may have important implications for synchronized beating and mechanical regulation of cardiac tissue.

2. Active Fluctuations in Living Matter: Extracting Work from Random, Nonequilibrium Motion

Random Brownian motion due to thermal agitation is well studied and familiar to material scientists working on fluids and soft matter. It is responsible for diffusion of molecules in fluids, the dynamic conformations and shape fluctuations of polymers and membranes, and a host of phenomena in soft matter. Within living matter, there are, in addition, active fluctuations, where random motion results from random active forces. Such forces arise from energy-consuming processes, which in living cells involve the use of chemical energy, such as in the form of ATP. The random active forces and motions in living systems have been revealed over the past two decades and seem to play important and varied roles. Note that we focus here on random active forces, which are distinct from the highly directed motion that is more often associated with active forces inside cells, for example as arises from molecular motors persistently walking along biopolymer tracks.

An important example of chemical energy conversion into active forces arises from the exothermic hydrolysis reaction of ATP in which the triphosphate molecule ATP in water dissociates into diphosphate ADP and a phosphate group.[2,5,6] Molecular motors such as myosin proteins convert the energy derived from repeated cycles of ATP hydrolysis into force and movement. Each Myosin II molecule has two globular heads containing both the actin binding site and the ATP binding and catalyzing site. During the mechanochemical cycle, myosin binds ATP and hydrolyzes it to ADP and an inorganic phosphate ion. The energy released from this chemical process is coupled to a conformational change of the motor that increases the affinity of the myosin head to actin. The release of the phosphate ion and the ADP molecule triggers the power stroke—a force-generating large conformational change in shape during which the myosin head is displaced and regains its original conformation, thereby advancing a certain step size (on the order of several nanometers) on the actin polymer "track" (see **Figure 1**).[21,23] At the end of the cycle, a new ATP molecule attaches to the myosin head reducing its binding affinity to actin and promoting motor detachment that allows repeating the cycle. In many cellular substructures, the myosin-II molecular motor has two "heads" connected by a rigid tail; each head tends to "walk" in the opposite direction along oppositely polarized actin polymers. Instead of "walking," such double-headed myosin molecules pull actin filaments, and the net accumulation of these steps can thus lead to contractions of the cytoskeleton network.[24]

Random active forces within cells can give rise to stronger mixing and stirring of the cytoplasm, leading to enhanced "active diffusion" of intracellular components.[25–27] Random active forces can on the one hand act to fluidize the cytoskeleton,[28,29] as observed in the oocyte[30] and bacteria,[31] while on the other hand they can cause large stresses to form that stiffen the cytoskeletal network.[32–35,48] Random active forces may affect the organization of chromatin, and thereby influence the expression of genes and the cell fate.[35–37] It is therefore clear that the random active forces can have very profound effects on the elastic properties of the cell, as well as provide forces that drive fluctuations and random motion.

Due to this dual effect of the active forces, which modify the elastic properties and provide a nonthermal source for motion, it is difficult to directly interpret experimental observations. Simplified theoretical models of activity, as presented below, are therefore essential for discriminating active random motion from thermal motion in living systems. These models also allow for the quantification of the active motion, and in many cases help to expose the underlying dominant biological mechanism.

© 2018 WILEY-VCH Verlag GmbH & Co. KGaA, Weinheim

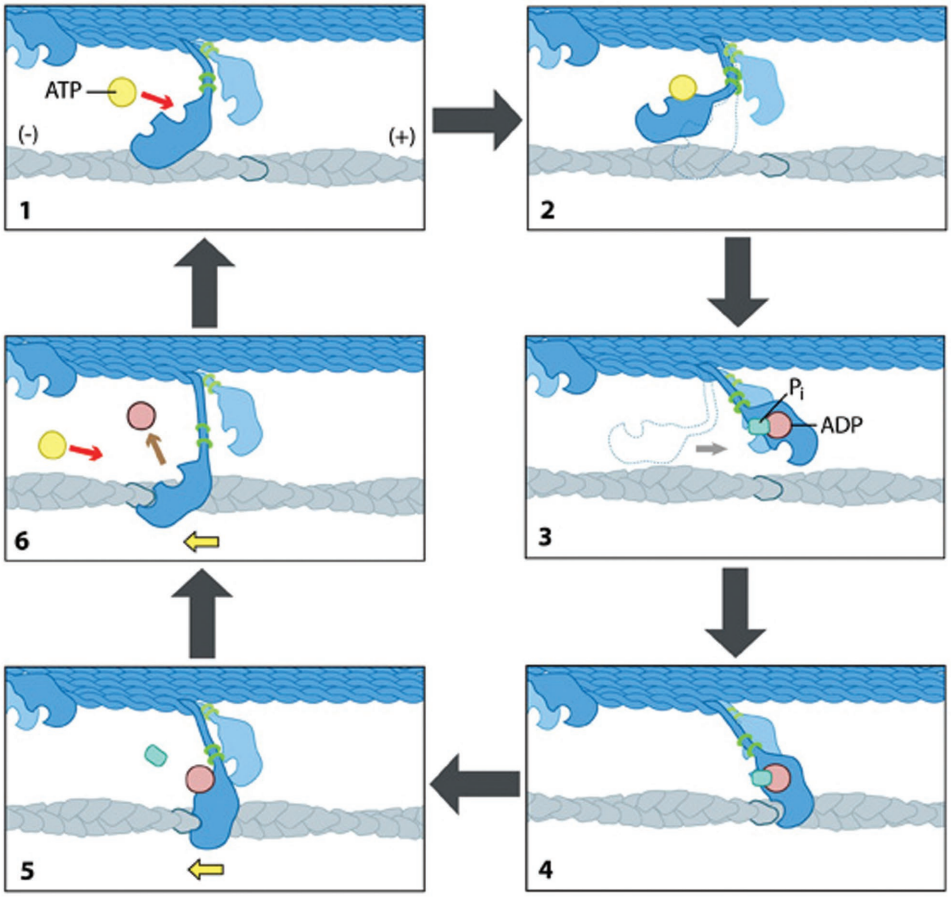

Figure 1. Myosin molecular motor (in blue) walking on a polar actin filament from its minus to its plus end (in gray). The various conformations of the myosin molecule are determined by whether it is bound to ATP or ADP. The energy released by the hydrolysis of ATP to ADP and a phosphate ion transfers energy to the myosin that facilitates its conformational change and ability to bind actin at a site different from its initial position. Reproduced with permission.[20] Copyright, Mechanobiology Institute, National University of Singapore. Image provided courtesy of the Mechanobiology Institute, National University of Singapore.

We first discuss the theoretical treatment of such active fluctuations, using simple models, to emphasize how they differ from thermal fluctuations. We then review several examples where random fluctuations have been investigated, from the simplest red blood cells (RBCs) and artificial membranes to more complex nucleated cells.

2.1. Simple Model for Active Fluctuations

We present here a simplified model for describing active fluctuations, which highlights the difference compared with thermal fluctuations. This model is later shown to be a useful framework for quantitatively describing active fluctuations in a variety of biological systems. By quantifying the active process that drives the fluctuations, this model can help identify the origin of the active forces, which are not easy to isolate in the complex living cell.

Note that the active fluctuations are sometimes treated as an "effective temperature," whereby the activity simply adds to the thermal temperature.[38–41] This treatment is valid for various purposes, but in general the active fluctuations do not behave as the thermal fluctuations, as shown below.

2.1.1. Fluctuation–Dissipation Relation (FDR) in Thermal Equilibrium

We start with a Langevin equation of motion describing the balance of forces acting on a point particle diffusing in a viscous fluid,[42] in one-dimension. In thermal equilibrium we have

$$\dot{v} = -\lambda v + f_{\mathrm{T}} \tag{1}$$

where λ is the friction coefficient; we normalized both sides by the particle mass and f_{T} is the thermal noise. The thermal noise is related to the friction coefficient since in thermal equilibrium the thermal bath that provides this noisy force is also the bath to which the particle loses energy in the form of heat due to friction. The relation is given by the expectation value of the thermal force correlations

$$\left\langle f_{\mathrm{T}}(t) f_{\mathrm{T}}(t') \right\rangle = 2\lambda k_{\mathrm{B}} T \delta(t - t') \tag{2}$$

From this relation it is clear that the thermal forces do not provide any particular force scale, or time scale, but rather are in the form of "white noise" that is only characterized by the energy scale $k_{\mathrm{B}}T$.

© 2018 WILEY-VCH Verlag GmbH & Co. KGaA, Weinheim

For this case, we can calculate the response of the particle to the perturbation of an external, periodically varying force: $f_{ex}(t) = Fe^{i\omega t}$, which results in a perturbation of the particle position: $\delta x(t) = \chi_{xx}(\omega)e^{i\omega t}$, where $\chi_{xx}(\omega)$ is the response function (the indices xx denote the response of the displacement due to a force that acts to displace the particle). The response and the displacement fluctuations $S_{xx}(\omega)$ are calculated in this simple model to be

$$\chi_{xx}(\omega) = \frac{1}{\omega(i\lambda - \omega)} \tag{3}$$

$$S_{xx}(\omega) = -\frac{1}{\omega^2} S_{vv}(\omega) = -\frac{1}{\omega^2}\left[\frac{2\lambda k_B T}{\lambda^2 + \omega^2}\right] \tag{4}$$

Substituting the expressions for the response (Equation (3)) and the fluctuations (Equation (4)), we find that they obey the fluctuation–dissipation relation in thermal equilibrium

$$k_B T = \frac{\omega S_{xx}(\omega)}{2\mathrm{Im}[\chi_{xx}(\omega)]} \tag{5}$$

2.1.2. Generalized FDR for Active Noise

In the active system, we also have in addition to the thermal noise an active noise[42]

$$\dot{v} = -\lambda v + f_T + f_A \tag{6}$$

We treat here active forces that have zero mean, $\langle f_A \rangle = 0$, and only provide an additional, symmetric noise term (see inset of **Figure 2**a).

The active forces are characterized by typical force and time scales. This is simply due to the underlying processes that produce those forces: the conformational change of the molecular motor, for example, is characterized by a given energy change and length of deformation. These limit the finite, maximal force that the motor can provide. There is also a typical time scale, either for the individual "power stroke" of a single motor activity event or for the duration of motor activity until it detaches from the biopolymer on which it is pulling. It is therefore natural to describe the active force correlations using "shot-noise" statistics of the form

$$\langle f_A(t) f_A(t') \rangle = p_{on} f_0^2 e^{-|t-t'|/\Delta\tau} \tag{7}$$

where f_0 denotes the average force that the motor produces, and $\Delta\tau$ is the average time over which the active force is applied, while individual active bursts have a Poisson distribution. The probability of the motor to be active is given by $p_{on} = \Delta\tau/(\Delta\tau + \tau)$, where τ is the mean waiting time between consecutive motor bursts. This may depend, for example, on the concentration of ATP.

The active noise does not modify the response that we calculated in Equation (3), but the displacement fluctuations now have an additional term

$$S_{xx}(\omega) = -\frac{1}{\omega^2}\left[\frac{2\lambda k_B T}{\lambda^2 + \omega^2} + 2N_m p_{on} \frac{f_0^2 \Delta\tau}{(\lambda^2 + \omega^2)(1 + \omega^2 \Delta\tau^2)}\right] \tag{8}$$

where the second term is due to N_m independent active "motors." We assume here that the random thermal and active forces are uncorrelated with each other.

Using these quantities, the response and the fluctuations, we can write a generalized FDR relation, which defines an "effective temperature" T_{eff} of the form[44]

$$k_B T_{eff}(\omega) = \frac{\omega S_{xx}(\omega)}{2\mathrm{Im}[\chi_{xx}(\omega)]} \tag{9}$$

Substituting the expressions we obtained from our simple model (Equations (3) and (8)), we get

$$k_B T_{eff}(\omega) = k_B T + 2N_m p_{on} \frac{f_0^2 \Delta\tau}{\lambda(1 + \omega^2 \Delta\tau^2)} \tag{10}$$

The first term is simply the "true" temperature, which is the only term in thermal equilibrium. However, the second term, which arises from the activity, is frequency dependent and makes the effective temperature frequency dependent: in the limit of high frequencies ($\omega \gg \Delta\tau^{-1}$) the active contribution is negligible and only thermal fluctuations dominate, while for slow fluctuations ($\omega \ll \Delta\tau^{-1}$, $\omega \to 0$) the activity contributes a finite additional agitation that can dominate over the thermal motion, see the inset of Figure 2a. The value of $T_{eff}(0)$ does not

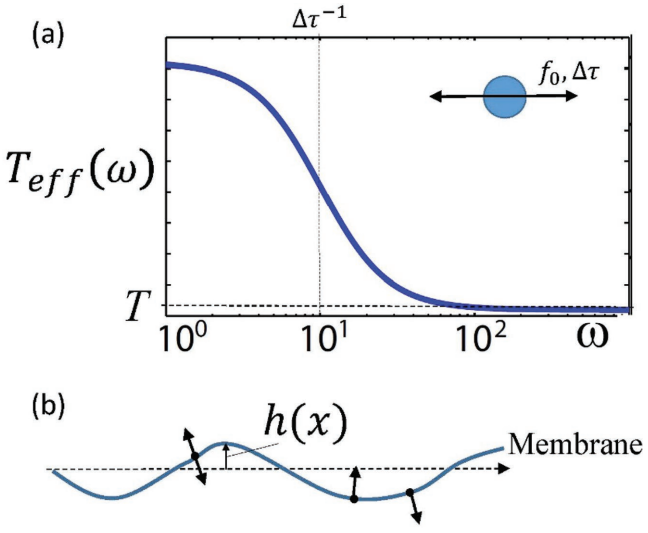

Figure 2. a) The effective temperature $T_{eff}(\omega)$ defined by the generalized FDR (Equation (9)), for the active particle in a viscous background (Equation (10)). At large frequencies ($\omega \gg \Delta\tau^{-1}$), the effective temperature approaches the thermal value T, while at low frequencies it approaches a finite value $T_{eff}(0)$. The inset shows the active random force, which is symmetric, has zero mean $\langle f_A \rangle = 0$, a variance given by Equation (7), and with persistence time $\Delta\tau$. b) An illustration of a membrane that develops undulations due to active force centers (arrows) that are either symmetric (on the left) or are asymmetric but occur with uniform distribution of both directions (on the right). The local membrane deformation is denoted by $h(x)$, making it natural to treat in terms of Fourier modes h_q, where q is the wavevector. Reproduced with permission.[42] Copyright 2011, APS.

© 2018 WILEY-VCH Verlag GmbH & Co. KGaA, Weinheim

in general agree with other measures of the activity, such as the extra kinetic energy arising from the active forces[42,71] Note also that when there is a wide distribution of time scales that control the activity, the value of $T_{\text{eff}}(0)$ may diverge (see Section 2.3.2).

Other variations of the simple model described above, such as the inclusion of an elastic restoring force, in the overdamped limit and for fluctuation modes of a continuous object (as opposed to a point particle), are briefly described below, in relation to specific examples of active systems.

The breakdown of the simple FDR was used in several experimental systems to conclusively reveal the active, nonequilibrium nature of fluctuations in cells,[45–47] as well as in reconstituted, in vitro systems.[48] Other schemes that expose the nonequilibrium nature of active dynamics, such as breakdown of detailed balance,[49,50] have been developed and recently reviewed.[51] The quantification of the departure from equilibrium due to activity and how to better characterize it are subjects of intensive current research.[52,53]

2.2. Active Fluctuations of Artificial Membranes and the Red-Blood-Cell Membrane

The cell membrane is the medium through which cells interface with the outside world. The membrane is therefore easier to probe than the internal cell cytoplasm since membrane shape fluctuations can be more easily monitored. Unlike the point particle considered in the equations above, the membrane is an extended object whose fluctuations are best described in terms of wave-like undulations. A similar treatment therefore also applies to the active fluctuations of other extended objects such as semiflexible filaments.[49,54–56]

2.2.1. Artificial Active Membranes

The membrane of cells contains several possible sources of active forces. The dominant one is probably due to the forces exerted on the membrane by the cytoskeleton of the cell, which usually contains a network of biopolymers (actin and microtubules) and their associated molecular motors. However, the study of the cytoskeleton–membrane coupling is difficult, especially in reconstituted systems, and therefore other and simpler sources of membrane activity have been experimentally explored. One such source, for example, is the activity of membrane pumps, whereby ATP is used to drive ions against the chemical gradient, establishing the electric potential across the cell's membrane. Active membranes that contain such ion pumps have been produced successfully,[57–59] and the contribution of the active forces to the observed membrane fluctuations was measured.

In order to compare the experiments to the simple model described above, it is more convenient to write the overdamped version (where the acceleration term in Equation (1) is neglected) and write an equation of motion for each mode of sinusoidal membrane undulation[60,61] (denoted by the wavevector q)

$$\dot{h}_q = -\omega_q h_q + f_{\text{T}}^q + f_{\text{A}}^q \tag{11}$$

where h_q is the amplitude of the membrane deformation at wavevector q, and ω_q is the corresponding membrane shape recovery rate; the last two terms account for the thermal and active noise as before. The active contribution to the mean-square amplitude of membrane deformations is given by

$$\left\langle h_q^2 \right\rangle = \left(\frac{f_0}{4\eta q} \right)^2 \frac{n}{2\omega_q \left(\omega_q + \Delta\tau^{-1} \right)} \tag{12}$$

where η is the viscosity of the fluid surrounding the membrane, and n is the density of active force sites on the membrane. Unlike thermal fluctuations, where the mean-square amplitude is $\left\langle h_q^2 \right\rangle = \dfrac{k_{\text{B}}T}{2\omega_q}$ and therefore a function only of $k_{\text{B}}T$ and the elasticity of the membrane (which appears in the formula for ω_q), the active contribution also depends on the dynamic properties of the system, such as the viscosity. This feature was observed in experiments using membranes containing ion pumps.[57] Another outcome of this model is that the temporal height–height correlation function has two terms[49,62]

$$C(q,t) = \frac{1}{\omega_q^2 - \Delta\tau^{-2}} \left(\mathrm{e}^{-t/\Delta\tau} - \frac{1}{\omega_q \Delta\tau} \mathrm{e}^{-\omega_q t} \right) \tag{13}$$

The distinct feature that the model predicts is a wavevector-independent peak in the measured correlation function (the first term in the bracket on the right-hand side of Equation (13)), which was recently observed in active membranes that contain rotary motors.[63]

Note that the active forces can also modify the elastic properties of the system, so that ω_q is dependent on the activity. For example, in the active membrane studies it was found that the activity changes the bending modulus and the tension in the membranes. In part, these effects are due to the larger fluctuation amplitude that renormalizes the elastic constants[2] and in part due to molecular-scale shape changes and interactions that change when the active proteins (ion pumps or rotary motors) undergo their activity cycles.

2.2.2. Active Fluctuations of the Red-Blood-Cell Membrane

The RBC is probably the simplest cell in our body, containing no internal organelles and lacking a cytoplasmic cytoskeletal network. The spontaneous fluctuations of the membrane of these cells were observed for decades and initially attributed to purely thermal agitation.[64] It later became clear that there is a dependence of the fluctuations on the metabolic activity,[65] but it remained as an open challenge to determine if there are active forces that contribute to the membrane deformation or is metabolic activity simply modifying the elastic properties of the system. It was indeed observed, as in artificial active membranes, that the RBC metabolic activity does modify the elastic properties of the membrane.[59,66] However, there were several experimental studies that clearly determined that active forces give a dominant contribution to the fluctuations of this system:

© 2018 WILEY-VCH Verlag GmbH & Co. KGaA, Weinheim

i. Whereas equilibrium systems generally show a Gaussian distribution of membrane displacements due to thermal fluctuations, active systems show a distinctly non-Gaussian distribution, but only in the presence of metabolic activity.[67] While this property could also arise from highly nonlinear elastic behavior, it was predicted to appear when active forces are present.[42,68]
ii. The additional relaxation mode, which is independent of the wavevector (Equation (13)), was detected in the dynamics of the RBC membrane (**Figure 3**a), only when metabolic activity is present.[62]
iii. Finally, the breakdown of the FDR was directly measured[45] (Figure 3b), definitely proving the active nature of the RBC membrane fluctuations.

What are the sources of active forces in the RBC membrane? One possibility is that these forces could arise from the activity of ion pumps, which exist in all cellular membranes. In addition, it was proposed that the network of proteins that cover the inner part of the RBC membrane may undergo ATP-induced reorganization that results in the local release of tension and the production of membrane-deforming forces.[69] This model was later elaborated upon in detail.[45]

The active fluctuations of the RBC membrane may therefore be a byproduct of the natural activity of ion pumps, which is essential for the osmotic stability of the cell. Alternatively, it may be a byproduct of the active reorganization of the membrane-bound cytoskeleton network, a process that is essential for maintaining the RBC soft and elastic so that it can flow through the narrowest capillaries in the body. The active fluctuations may also serve to stir the cytoplasm, which can aid in mixing of the hemoglobin for better oxygen binding.

2.3. Active Fluctuations within Acto-Myosin Gels and inside the Cell Cytoplasm

The cytoplasm of nucleated cells is filled with a network of biopolymers, which comprise the cytoskeleton. This network endows the cells with their viscoelastic properties, determine the cells' shape, and serve as conduits for molecular motor traffic throughout the cell. One major component of the cytoskeleton is the network of actin filaments which is crosslinked to form a gel and undergoes contractile motions due to myosin-II motors that adsorb to the actin filaments. We are interested here in the active *random* fluctuations within such a cytoskeletal network,[70] as opposed to the highly coordinated global contractions that occur, for example in muscle or heart cells (see Sections 4 and 5).

2.3.1. Active Fluctuations of In Vitro Acto-Myosin Gels

Since it is quite difficult to probe the active fluctuations within the cytoplasm, there have been a number of studies of the dynamics of connected actin networks ("gels") that contain myosin-II motors, in vitro. The fluctuations within such a system, as revealed by the motion of a passive tracer particle embedded in the gel,[33,48] may be described by an extension of the simple model described above[71]

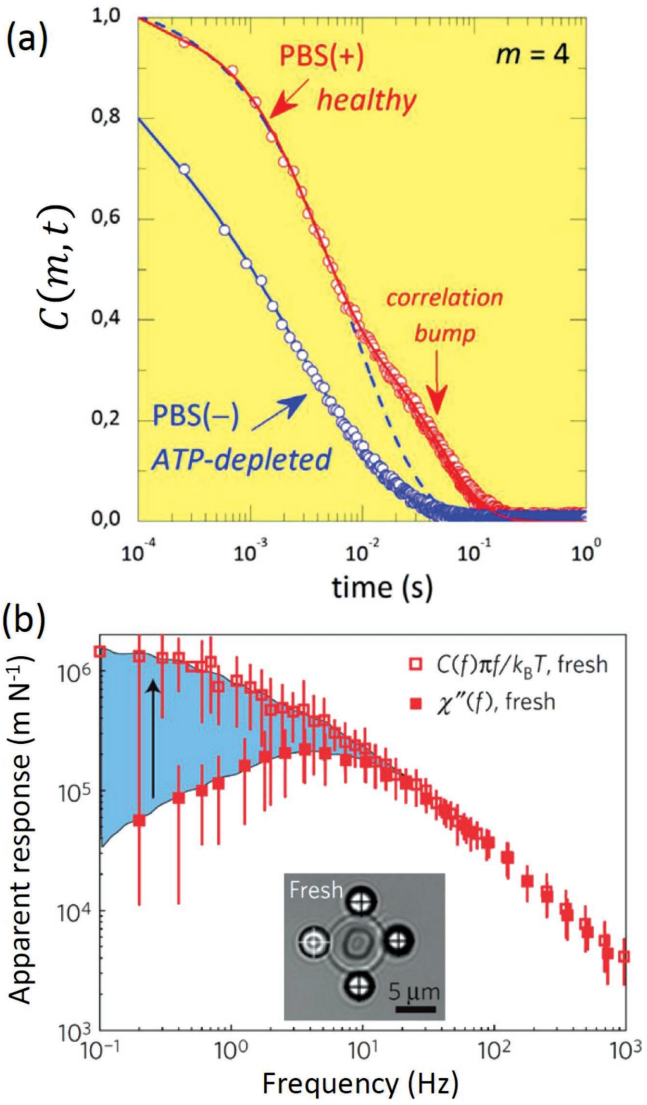

Figure 3. a) Comparison between the membrane temporal height–height autocorrelation function (for mode number $m = qR_{RBC} = 4$, Equation (13)) in passive cells (blue) and in healthy cells (red) (lines give the theoretical fits to the experimental data in circles). Membrane fluctuations and apparent response. Reproduced with permission.[62] Copyright 2015, Elsevier. b) For fresh RBCs, the measured response (filled red squares) and the response calculated from fluctuations measurement (displacement power spectrum density $C(f)$, open red squares, where f is the frequency) differ below 10 Hz by more than an order of magnitude, indicating a clear violation of the FDR (Equation (5)). Reproduced with permission.[45] Copyright 2016, Springer Nature.

$$\dot{v} = -\lambda v - kx + f_T + f_A \tag{14}$$

where k is the spring constant of the surrounding network. Note that in this system there is another time scale, which is the natural oscillation frequency of the tracer particle in the confining elastic network.

This model is valid for the periods where the tracer particle was observed to be "trapped" around a specific location. On long times, the tracer performs a "hopping"-type motion, where the surrounding network undergoes a rearrangement that allows

© 2018 WILEY-VCH Verlag GmbH & Co. KGaA, Weinheim

the tracer to move to a new location in the network. The long-time limit motion is therefore diffusion within a viscous fluid, but on short time scales the elastic nature of the actin network can be described by the harmonic confinement of Equation (14).

Using Equation (14) we find that in this system our model predicts highly non-Gaussian distributions of the tracer position within each trapping site, and therefore non-Gaussian van-Hove distribution of the displacement–displacement correlations. The model predicts that under conditions of a stiff actin network, the van-Hove distribution should exhibit distinct side peaks that correspond to the motion induced by individual motors. Surprisingly, this simple model predicts that $T_{\text{eff}}(\omega)$ as found from the generalized FDR (Equation (9)) is independent of the network stiffness k.

Comparing this model to the observed deviation from the FDR,[48] we can extract the mean active burst duration (Equation (7)) $\Delta\tau \approx 100$ ms and magnitude of $\frac{T_{\text{eff}}(0)}{T} \approx 20-100$. The non-Gaussian nature of the van-Hove distribution was also observed in experiments,[72] and by comparing to the model one can extract similar estimates for the time scale and amplitude of the active forces.

2.3.2. Active Fluctuations of the Cell Cytoplasm

Probing in a direct manner, the fluctuations within the cytoskeleton of a living cell is a difficult challenge. Earlier works exposed the active nature of these fluctuations indirectly, by attaching a tracer bead to the cell membrane and observing its motion.[73,74] The observed motion in these cases is a measure of the fluctuations of the cell membrane which are driven by membrane active processes (see the previous section), activity of the cortical cytoskeleton of the cell, as well as the cytoskeleton within the cell bulk.

One method to directly probe the fluctuations within the cytoplasm of a living cell was reported in,[46] using the injection of fluorescent beads that have been treated to prevent strong binding with the cellular constituents. The trajectories of the beads were recorded, to give the fluctuations (**Figure 4**a), while laser tweezers were used to probe the response function of the cytoplasm. Combinedly, the breakdown of the FDR at low frequencies can be obtained (Figure 4b) using Equation (9).

Using the overdamped version of Equation (14)

$$\dot{x} = \frac{1}{\lambda}\left(-kx + f_{\text{T}} + f_{\text{A}}\right) \tag{16}$$

We can relate the spring constant k to the measured bulk modulus of the cell. Since in our model the response function is given by $\chi_{xx}(\omega) = 1/(\text{i}\omega\lambda + k)$, we can relate it to the complex bulk modulus

$$G^{*} = \frac{1}{6\pi a \chi_{xx}} = \frac{k}{6\pi a} + \text{i}\omega\eta = G' + \text{i}G'' \tag{17}$$

Here, G', G'' are the real and complex components of the bulk modulus, respectively, which can be obtained from the measured response of the beads when an external oscillatory force is applied to them by laser tweezers. Using this identification, it was shown that the scaling dependence of the mean-square displacement (MSD) on the bead size, for example, can be explained by the model.[46] The power spectrum of the force fluctuations is observed to decay as ω^{-2} at low frequencies, which is a common feature of the active noise models: the force equals the velocity in the overdamped regime and the power spectrum is therefore given by $S_{vv}(\omega)$ (Equation (8)).

In order to account for the long-time scale viscous behavior of the cytoskeleton, whereby long-range diffusion of the tracer bead is observed, an elaboration of the original model was proposed.[47,75] In this model, the motion of the tracer particle is divided into purely thermal fluctuations within a harmonic confining potential, while the activity is manifested by occasional bursts of force that move the confining potential to a new spatial location, dragging the tracer along. The translational motion of the confining potential represents the reorganization of the cytoskeletal network around the tracer particle, due to the active force. The equations of motion have this (overdamped) form

$$\dot{x} = \frac{1}{\lambda}\left(-k(x - x_0) + f_{\text{T}}\right) \tag{18a}$$

$$\dot{x}_0 = \frac{1}{\lambda} f_{\text{A}} \tag{18b}$$

This division between the thermal and active motion is phenomenological, based on the difference in time scales between

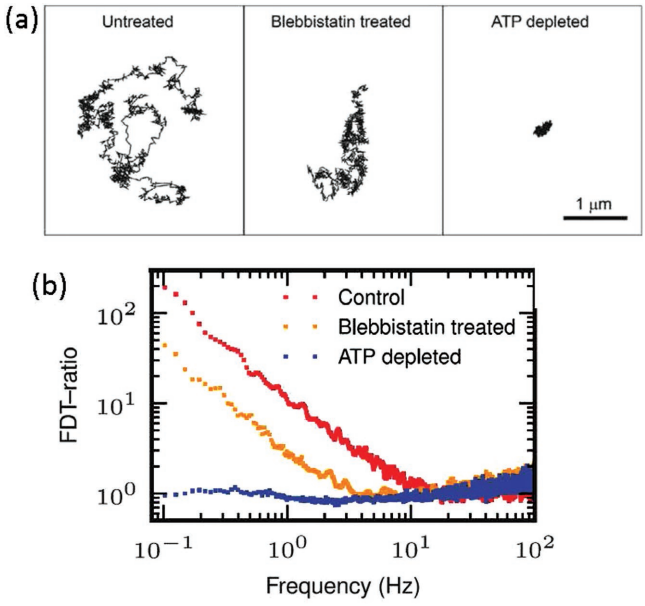

Figure 4. a) Typical trajectories of 200 nm PEG-coated beads in A7 cells under three conditions: control, 10×10^{-6} M blebbistatin treatment (which inhibits the activity of myosin-II molecular motors), and ATP depletion. The trajectory length is about 2 min. b) Generalized FDR ratio (i.e., $T_{\text{eff}}(\omega)$, Equation (9)) as a function of frequency. It equals 1 in ATP-depleted cells as for an equilibrium system, and it deviates from it in the two other conditions at small frequency showing that nonequilibrium processes drive the dynamics in this regime. Reproduced with permission.[46] Copyright 2015, IOP Publishing.

© 2018 WILEY-VCH Verlag GmbH & Co. KGaA, Weinheim

the rapid thermal agitation and the slower active motion. Note that the friction coefficient for the motion of the location of the trap, x_0, is not well defined, as it is the friction of the motion of the network surrounding the tracer.

However, this framework simplifies the analysis and provides excellent description of the observed motion within an egg cell (oocyte).[47] In this system, the tracer particles that are tracked and used to probe the response are naturally occurring passive vesicles,[30] thereby eliminating the need to inject external beads (as was done in ref. [46]). The bulk modulus of the oocyte was found to have a complex frequency dependence, and similarly the friction coefficient λ is replaced by a time-dependent memory kernel in Equations (18). The effective temperature defined from the generalized FDR (Equation (9)), $T_{\text{eff}}(\omega)$, was found to diverge in the $\omega \to 0$ limit.[46,47]

Beyond explaining the qualitative features of the observed active fluctuations, and scaling relations, the theoretical model described above can be used to extract the characteristics of the active forces from the experimental data. This is important since within living cells it is difficult to isolate the dominant mechanism that drives the active motion. By comparing the force scale and the time scale of the activity which is obtained by fitting the model to the observed data, the most likely candidate molecular motor, for example, can be revealed. In the cytoplasm of regular cells it is found that myosin-II contributes the dominant source of active fluctuations,[46] while in the cytoplasm of the oocyte it turns out that myosin-V plays the major role.[47] Recently, this same model was used to quantify the active fluctuations on a larger scale, at the cell-cell junctions in a confluent multi-cellular tissue.[76]

2.4. Inhomogeneous Active Fluctuations and Directed Motion

So far we have discussed systems where the active fluctuations can be approximately treated in terms of an increase in the effective temperature. We now show that there are cases where this simple picture does not hold.

What happens when the active fluctuations are not spatially uniform? If one treats the active fluctuations as an effective temperature, such a thermal gradient will cause a gradient in the density of the system so that at steady state the pressure will become uniform throughout. A passive object placed in this system should therefore not feel any net force due to the thermal gradient (ignoring thermophretic effects). However, active particles, driven by nonthermal random noise, have a characteristic persistence time $\Delta\tau$ (Equation (7)), and therefore behave very differently from particle diffusing due to thermal noise (Equation (2)). Near boundaries, the persistent active particles tend to accumulate, which is different from the uniform distribution of particles diffusing in thermal equilibrium. This accumulation determines the behavior of a passive object placed in a bath of active particles that have a spatial gradient in their activity.

Active particle ratchets, in which the force applied by active particles to objects is used to perform work, have been implemented both in experiments and simulations.[77–79] In systems containing active particles, the forces these self-propelled particles (SPPs) exert may be used to perform work. This was shown in both simulations and experiments.[78,79] However, in order to extract work from such nonequilibrium systems it is necessary to break time reversal and space inversion.[80,81] The time-reversal symmetry is broken by the persistent motion of the SPPs and their interaction with external boundaries and passive objects, while the space inversion symmetry is often broken using a special geometry for the boundaries or the passive objects. The activity, however, is usually uniform in all these systems.

The motivation to study a nonuniform activity comes from the observation of the random motion of active vesicles within the oocyte (**Figure 5**a), whose mean-square velocity $\langle v^2 \rangle$ was observed to increase from the cell center to the cortex.[30,47] This gradient in activity, combined with the rather uniform density of actively moving vesicles, was suggested to provide an effective pressure that acts on the nucleus of the oocyte, pushing it from the cortex to the cell center (Figure 5b). Since the density of active vesicles is uniform, the net force acting on a passive object should naively be proportional to the gradient in $\langle v^2 \rangle$ (Figure 5c).

This proposal was recently systematically explored using a model of SPPs[43,82] where the activity has a gradient either in the intrinsic active velocity of the particles ($v_0 = f_0/\lambda$, Equation (7)) or in the persistence time of the motion, $\Delta\tau$. Note that the experimental measurement of a gradient in $\langle v^2 \rangle$ is not necessarily indicative of a gradient in the intrinsic velocity of the SPPs since the measurement time was of the order of the persistence time.[82] It was found that the effect of a gradient in these two properties of the activity is very different: a gradient in the persistence time allows for a uniform density of particles, but predicts that the different accumulation of the SPPs on the surface of the passive object drives the net force acting on it. On the other hand, a gradient in the intrinsic driving force gives rise to a strong density gradient since at steady state the density is inversely proportional to the SPP velocity: $\rho(r) \propto c/v(r)$. The accumulation of SPPs on the surface of the passive object is now uniform, but the gradient in pushing forces gives rise to a net force.

An interesting result is that in the limit of short persistence times, such that the persistence length of the SPPs, $l_p = v_0\,\Delta\tau$, is much smaller than the size of the cell or the pushed object (nucleus of the oocyte), the net force on the passive object obeys an Archimedes-like relation

$$F_{\text{tot}} \propto -c\frac{\partial l_p}{\partial x}V_{\text{ob}} \tag{19}$$

Here, V_{ob} is the volume of the passive object (or area in a 2D problem), the constant $c = \rho(r)v(r)$, $\rho(r)$ is the local density of SPPs and $v(r)$ is their local velocity. The gradient in the activity plays the role of gravity in the case of buoyancy (the original Archimedes system). In the oocyte it is estimated that $l_p \approx 0.2$ μm, which is indeed much smaller than the nuclear diameter of ≈10 μm and the cell diameter of ≈70 μm.

Returning to the oocyte system, this theoretical study may indicate that the gradient in activity is most likely imposed through a gradient in the persistence time, which agrees with the observed uniform density of vesicles. Note that the active vesicles are driven by myosin-V motors that move on a randomly oriented network of actin filaments. It is not known at present what is the mechanism that produces the gradient

© 2018 WILEY-VCH Verlag GmbH & Co. KGaA, Weinheim

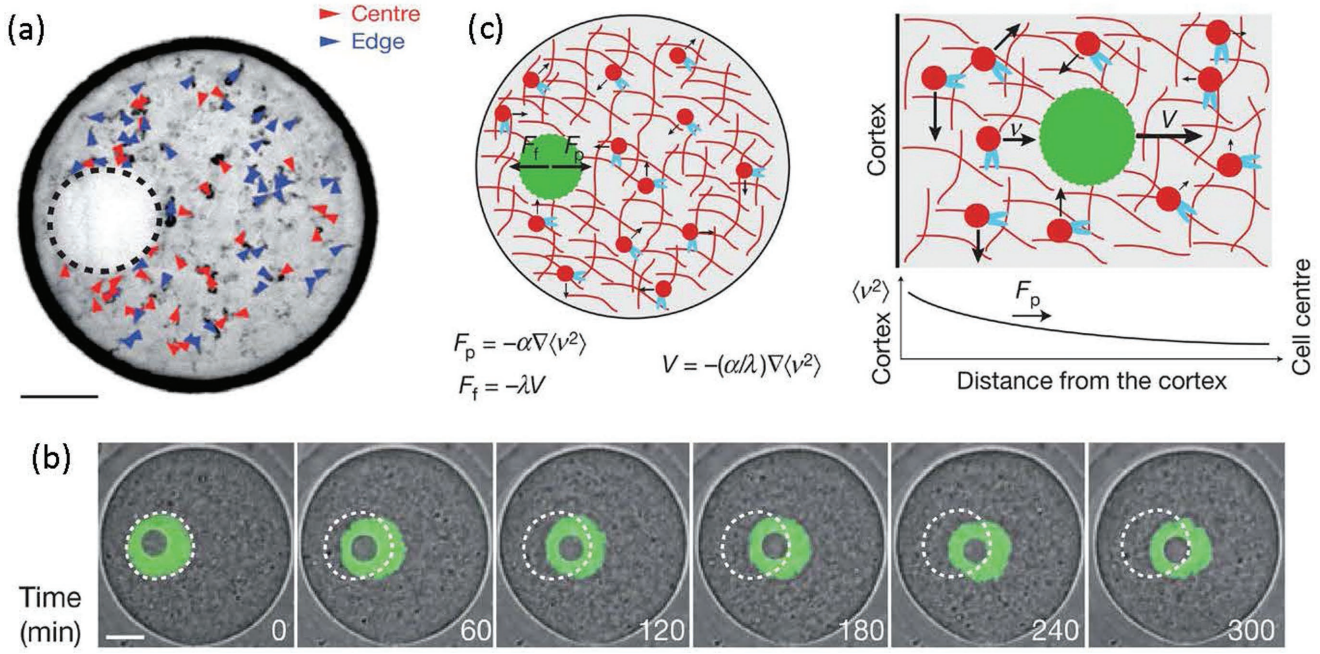

Figure 5. Dynamics of active vesicles in the oocyte. a) A single snapshot from the experiment, where the motions of the actin-covered vesicles are denoted by the arrowheads (red toward the cell center, and blue away from the center). The nucleus is marked by the dashed line (scale bar: 15 μm). b) Series of images demonstrating the motion of the nucleus from the cell cortex to the center. The nucleus is marked by a nuclear probe (in green). c) A schematic illustration of the force imbalance that pushed the nucleus to the center due to a gradient in activity: the propulsive force is $F_p \propto -\nabla\langle v^2\rangle$ due to the gradient in the motion of the myosin-Vb-driven vesicles. This gradient vanishes at the cell center, thereby maintaining the nucleus in this position. The propulsive force is balanced by a drag force denoted by F_f. In this illustration, the nucleus is represented by the green circle, actin-coated vesicles by the red dots, actin filaments by red lines, and myosin-Vb motors are represented by blue dots. Reproduced with permission.[30] Copyright 2015, Nature Publishing Group.

in the motor persistence time across the cell, but it may be due to a structural gradient in the actin network or some chemical gradient that controls the motor activity.

3. Cellular Reconstitution of Self-Contracting Poroelastic Actomyosin Sheets

This section focuses on cellular reconstitution of acto-myosin contractility in vitro. Physics has a long tradition of studying material properties and many tools and concepts have been developed in this context. These are now being applied to living cells, which—due to their nonequilibrium character—pose new challenges compared to the studies of conventional, "dead" (equilibrium, nonactive) materials. Living cells control their shape and mechanical properties via the active reorganization of their cytoskeletal networks. Yet, due to the complexity of the in vivo cellular environment, the direct effect of a given parameter on cellular reorganization, or any other cellular process, is practically impossible. For that purpose, in vitro reconstitution systems were developed.[83,84] Due to their simplicity and their well-controlled nature, these systems enable us to study effects such as system geometry, molecular composition, and the effect of externally applied forces. Moreover, the data extracted from such experiments can be used for physical modeling. Overall, the main challenge is to develop systems that are simple enough to enable full control of their parameters, which is essential for quantitative studies. Yet, they should have sufficient degree of complexity to allow faithful representation of a known, biological function. In that way, in vitro systems can provide complementary information to live-cell studies.

Below we describe the dynamics of contraction and buckling of thin poroelastic acto-myosin gel sheets as a model system for active, contractility generated shape transformations in developing tissues.

3.1. Self-Contracting and Buckling of Poroelastic Acto-Myosin Sheets

A central property of developing plant and animal tissues is their ability to form a diversity of folded patterns and to adopt curved shapes through mechanical instabilities that break the planar symmetry of growing epithelia.[14,85–87] The folding of growing epithelia can result from external mechanical constraints that restrict in-plane expansion.[88] Morphological changes can also occur in unconstrained sheets,[89] where the emergence of wrinkles is associated with excess growth of the margins relative to the center of the sheet. This mechanism explains the shape of leaves and flowers.[89–91] In contrast to the shaping of growing tissues, the deformation of animal embryos during gastrulation often proceeds largely in the absence of tissue growth and relies on active contractility.[14–16] In most cases, the mechanisms that are responsible for tissue folding are usually studied in cell epithelia (layer(s) of cells). In that

© 2018 WILEY-VCH Verlag GmbH & Co. KGaA, Weinheim

case, shape deformations have been observed, when a contractile epithelium was subjected to anisotropic contraction[92] as well as in the case when it was coupled to an elastic substrate.[15] This presents a major difficulty for studying the intrinsic effect of actomyosin contractility on tissue folding in vivo where the external deformations and substrate cannot be controlled.

In recent work, we show that suspended, contractile actomyosin gel sheets can provide a good model system for studying contraction-induced folding.[9] We show that contractile actomyosin gel sheets behave as a poroelastic material, where a flow of fluid is generated during contraction. We also observed that the acto-myosin sheet can spontaneously buckle and that the buckling instability resulted from system self-organization and the spontaneous emergence of density gradients driven by the active contractility. These new findings demonstrate that buckling can be spontaneously generated by myosin activity and does not require mechanical coupling to the environment or *preimposed* gradients in the material properties of the sheet. The latter effect has been shown to be responsible for buckling in synthetic systems prepared with inhomogeneous crosslinkers densities or elastic moduli.[93] Below we discuss the main findings of this study.

We fabricated symmetric, circular thin suspended contractile elastic acto-myosin sheets of controllable extent and elastic properties[9] by polymerizing actin in the presence of the strong passive crosslinker fascin and clusters of myosin II motors that act as active crosslinkers. Contractile elastic gels formed only if actin polymerization occurred in the presence of the motors and passive crosslinkers.[94–96] The polymerization process was performed in chambers with a high aspect ratio. Specifically, the sheets had initial radii R (lateral extension) of about 1/2 cm and an initial thickness h of typically a hundred micrometer (vertical extension). This corresponds to an aspect ratio $R/h \approx 50$. The actomyosin gels spontaneously contracted through the activity of myosin motors with no need for external stimuli, save for the presence of ATP in solution. Contraction occurred only above a myosin concentration threshold.[95] For lower concentrations, the mechanical stresses generated by the motors were apparently too weak to overcome the gel's elasticity, whereas for higher motor concentrations the gel ruptured.[95,96]

The anisotropy in the gel extensions decoupled the contraction processes in the vertical and lateral directions. Namely, contraction started in the vertical direction and only when vertical contraction was essentially terminated, the contraction began along the lateral direction, thereby generating 2d actomyosin gel sheets of finite thickness. We found that during lateral contraction, the sheet thickness remained essentially constant. The actomyosin gels thus correspond to materials with an effective Poisson ratio $\nu \approx 0$; as discussed below, this is due to the flow of water out of the material as it contracts which is the signature of poroelasticity[10,12] of combined fluid flow and gel deformation as opposed to gel elasticity alone. At advanced stages of planar contraction, the sheet spontaneously started to buckle. The buckling instability resulted from system self-organization and was due to the spontaneous emergence of density gradients (highest at the gel edge and lowest at the center) driven by the active contractility that persisted in steady state. Buckling occurred when contraction of the gel periphery could not follow the contraction in the gel bulk. This

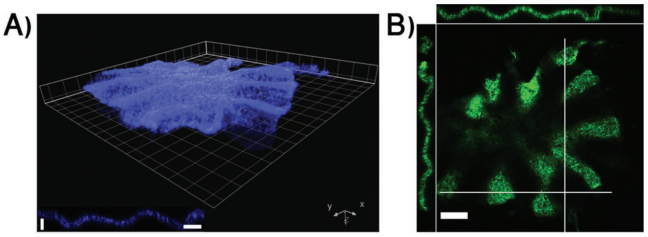

Figure 6. Buckling of an acto-myosin gel sheet. A) Laser scanning confocal microscopic image of a 3D view of a buckling gel at steady state. B) Laser scanning confocal fluorescence microscopic images of the actin gel in (A) in the *xy*-plane (top view), the *xz*-plane (top side view), and the *yz*-plane (left side view). Side views (*xz*- and *yz*-planes) are measured along the white lines. Scale bars: 100 μm (horizontal) and 60 μm (vertical) (insets of (A)) and 200 μm B). The grid mesh size is 100 μm (A). Reproduced with permission.[9] Copyright 2018, Springer Nature.

is reminiscent of surfaces under the constraint of a fixed perimeter that is longer than the perimeter of a circle of the same surface area. The emerging folds were directed perpendicular to the boundary and had a roughly sinusoidal shape (see **Figure 6**). The characteristic wavelength of the folded pattern was proportional to the sheet thickness, e.g., for a sheet thickness of ≈20 μm with a corresponding wavelength of ≈200 μm. Note that the macroscopic buckling phenomenon shown here occurs on a much larger length scale compared to the mesh size of the gel (≈10 μm at the end of the contraction process) and does not result from the buckling of individual filaments observed in dilute actomyosin networks in the presence of weak crosslinkers such as α-actinin.[97–100]

To obtain a better understanding of the system dynamics, we characterized the material properties of the system during lateral contraction taking into account the actomyosin network, the active stresses generated by myosin motors, and the aqueous phase within the gel. The circular sheets contracted isotropically throughout the process. This is in line with observations made on contracting actin gels that are attached to the surrounding inactive gel at the periphery, where motors have been activated by light in specific areas and where it was shown that the final state presents the same aspect ratio as the initial state.[101] Contraction began at the gel boundaries, which is a consequence of the initially homogenous distribution of motor-induced force dipoles (a myosin II motor exerts equal and opposite forces on the actin—see Section 3), which generated a homogenous active stress since the active, dipolar forces canceled each other (on average, at large scales) everywhere except at the boundaries. The contraction at the boundary resulted in an increase of the gel density at the periphery that later propagated into the gel interior with a characteristic time scale ranging between 20 and 40 s, so that stress relaxation occurs on time scales of 1–2 min. By analyzing the solvent flow during the gel contraction dynamics we found that a flow of the (penetrating) solvent was generated during gel contraction, thereby demonstrating that the actomyosin gels behave as poroelastic[10,11] active materials, as previously proposed for actin gels in living cells.[12,13] The fluid flow was (on average) opposite in direction to the motion of the contracting gel as shown in **Figure 7**. The magnitude of the flow (determined by the radial velocity v_r of beads added to the solvent), however,

© 2018 WILEY-VCH Verlag GmbH & Co. KGaA, Weinheim

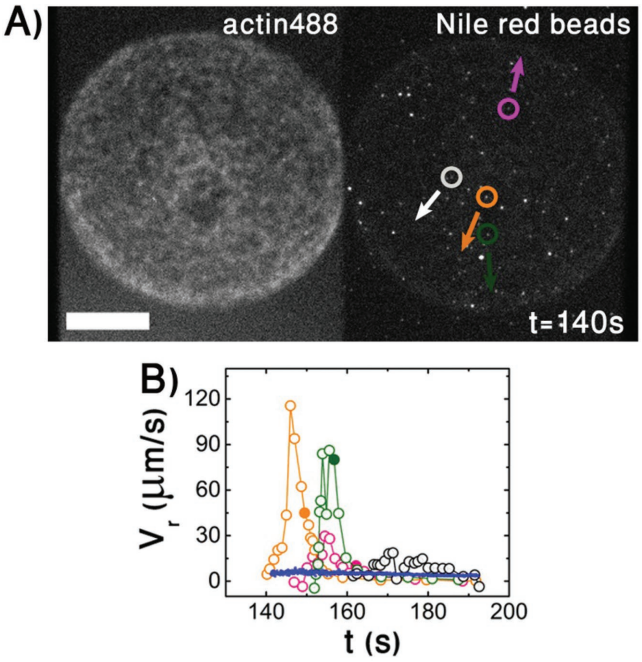

Figure 7. Acto-myosin sheets are poroelastic. A) Subsequent epifluorescence microscopic images of a contracting gel with embedded fluorescent beads with a diameter of 2300 nm at low magnification. Circles mark the positions of four beads shown in (B). Arrows mark the global direction of beads motion. Actin was labeled with Alexa-Fluor 488, and beads with Nile red. Scale bar: 400 μm. B) Radial velocity v_r of the same beads and of the gel edge (blue dots). The filled circles indicate the time, when the beads left the gel. Reproduced with permission.[9] Copyright 2018, Springer Nature.

depended on the relative volume fractions of the gel and the penetrating fluid and was always larger than the gel contraction velocity (by a factor of up to 20) as shown in Figure 7B. We further confirmed the poroelastic nature of our system by showing that (elastic) stress relaxation can be determined by an effective poroelastic diffusion constant D, which is proportional to an effective, concentration-dependent gel elastic modulus κ and inversely proportional to an effective friction constant γ that accounts for the permeation of water through the actin network such that $D \approx \kappa/\gamma$. Using a theory of actively contractile poroelastic gels, extended to include the nature (catch-bond behavior) of myosin motors[102] to increase the total force they can generate under enhanced elastic stresses, we confirmed the poroelastic nature our system and explained the observations and the physical basis of the contraction dynamics.

The overall motivation of this work was to shed light on macroscopic shape changes of 2D tissues observed in various (biological) systems induced by myosin contractility, for example, gastrulation in developing embryos,[14–16] and to show that purely physical mechanisms can underlie these transformations. Yet, the role of poroelasticity on the observed shape transitions remains to be demonstrated. We do expect though that the generation of a fluid flow due to contractility is a generic phenomenon, governing cellular processes, such as cell blebbing[13] and motility.[103] In fact, it is becoming increasingly clear that in many biological phenomena the mechanics of the cytoskeleton and cytosol are intimately intertwined and cannot be treated as separate entities.[104]

With respect to applications these bioinspired active materials can be used for generating active self-organized 3D structures of defined shape. They may also find applications as biomaterials that can improve human health. In particular, 2d intrinsically contractile sheets may be used as actively functional band aids that speed up wound healing or in form of beating patches that could support heart function.

4. Elastically Mediated, Active Interactions within and among Cells

In this section, we present a theoretical description of how active contractility of either acto-myosin segments within a single cell or entire, contractile cells themselves can result in elastically mediated interactions that lead to structural order within or among cells.[21,105] Within many cells there are acto-myosin contractile units that are adhered either to an underlying elastic substrate or to the gel found in the cell interior known as the cytoskeleton (see **Figure 8**). Experiments that probe cellular mechanics are often performed on soft elastic gels that match the Young's modulus of the cell (in the kPa range and thus smaller by orders of magnitude than that of crystals).[8,17,19,20,106,107] These mimic the crosslinked biopolymers (e.g., collagen or fibrin) that comprise the gel-like, extracellular matrix (ECM) in cell assemblies, which provides structural support to cell assemblies and tissues.[23] Thus, contractile cells within these soft, elastic matrices can interact via their mutual elastic deformations of surrounding gel.[21,108,109] In the synthetic materials context, this is analogous to the behavior of inclusions in solids (for which the different thermal expansion of the inclusion can result in contractile or tensile forces as the temperature is varied) or interstitial atoms in crystals (e.g., hydrogen in metals, where the different ion sizes can result in elastic forces) with the important difference lying in the active, nonequilibrium nature of cell contractility as explained below.[22,109,110]

Not only are elastic interactions important for the interactions of cells in and on gels, but a single cell itself responds elastically to external mechanical forces. These are transmitted to the cell via its adhesion to its elastic environment (see Figure 8); the adhesion complexes are linked, on their other end, to the cellular cytoskeleton either near the cell surface

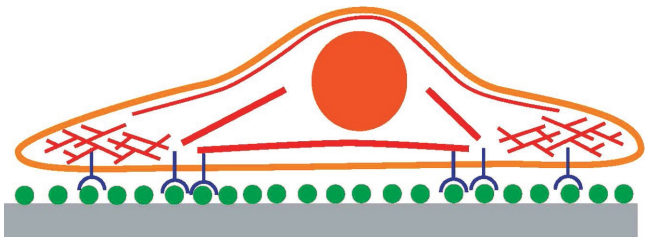

Figure 8. Schematic drawing of an adherent animal cell. Such a cell typically has the shape of a fried egg, with the nuclear region protruding in the middle while the rest of the cell remains relatively flat. In addition to the fluid lipid membrane (outer orange line) which is attached by proteins to the viscoelastic actin cortex (red on the top surface), the actin cytoskeleton (red crosshatch within the cell) includes both crosslinked actin as well as contractile actin filament bundles (stress fibers are shown by thick red lines) that are anchored to the cellular environment through transmembrane adhesion molecules (blue) that bind extracellullar ligands (green). Reproduced with permission.[21] Copyright 2013, American Physical Society.

© 2018 WILEY-VCH Verlag GmbH & Co. KGaA, Weinheim

(actin cortex) or in its interior (cytoplasm). The cytoskeleton comprises crosslinked polymers (e.g., actin, but also others) whose self-assembled structure is modified by the transmitted forces.[111,112] The cytoskeletal shear modulus[113] gives adhered cells their shape integrity, i.e., the cytoskeleton in an adhered cells responds to external mechanical forces by shape deformations (including reorientations).[21,108,111,114] The crosslinked cytoskeletal gel, while not translationally ordered as are crystals, still behaves mechanically as a solid and has a nonzero, albeit relatively small (compared to crystals), shear modulus.[115] For motile cells, this shear modulus is only nonzero on short time scales of seconds, while for well-adhered cells, the cytoskeleton may show an elastic response on significantly longer time scales that can be up to about an hour.[105,106]

As mentioned in Section 1, in adhered cells, myosin motors exert equal and opposite, contractile forces on two, antiparallel actin polymers that are adhered to the underlying substrate or 3D matrix. A simple, physical representation of a single acto-myosin, contractile unit is that of a force dipole (two equal and opposite forces separated by a small distance that represents the myosin "tail" length) in an elastic medium.[21,116–118] The mutual deformations of medium by two nearby force dipoles give rise to attractive or repulsive interactions between the contractile units that can act to change their separation; if they are well adhered to the matrix and cannot translate, they still can rotate and change their relative orientations.[17–21] The force dipole concept is multiscale and can also apply to entire cells, each modeled as a coarse-grained, contractile unit that interact via their mutual deformations of the substrate or 3D matrix.[21,110,116,119] We note that in contrast to electric or magnetic dipoles that are vectors, the force dipole is a tensor: $\boldsymbol{p}_{ij} = \boldsymbol{f}_i \boldsymbol{r}_j$, where $\boldsymbol{f}_i$ is the ith component of the vector force exerted by each dipole and $\boldsymbol{r}_j$ is the jth component of the vector distance between the two forces (two myosin heads).

4.1. Interactions and Ordering of Cellular Active Force Dipoles

Interactions of inclusions in solids via their mutual deformations of the intervening elastic medium is a classic effect that has been studied both theoretically and experimentally in materials science.[22,109] Each inclusion is acted upon and acts upon the matrix deformation induced by the other inclusion, giving rise to interactions that can be either attractive or repulsive. The deformation energies of both the inclusions and the elastic matrix are included since both are assumed to be in equilibrium and to respond in a similar manner to forces; the deformation due to the expansion or contraction of each inclusion (e.g., via thermal expansion—if the temperature is varied) results in a force on the inclusion exerted by the matrix. The interaction energy of two inclusions is then determined by the sum of i) the energy cost of deformation of the matrix and ii) the energy gain of the inclusion, proportional to the force exerted by each inclusion multiplied by the local matrix displacement. A simple analog is that of a spring (the matrix) stretched by a weight, hung over a pulley and acted upon by gravity (the inclusion). The latter accounts for the inclusion energies, analogous to the gravitational energy of the weight. These energies depend on the relative distance and orientations of the inclusions and can result in forces that tend to rotate or translate these bodies.[118]

However, in treating the case of active acto-myosin contractility, the molecular motors (and on a larger scale, cellular mechanosensing) are not in equilibrium and the energy they gain in deforming the matrix (analogous to the weight) is irrelevant. Thus, the only energy that should be included in calculating the interaction of two acto-myosin units (or two entire, contractile cells) is the matrix deformation.[21,119–121] This is indeed coupled to the active contractility by cellular adhesions that couple the cytoskeleton to forces within a gel-like matrix or substrate. The most important difference between the active and passive cases, is that the sign of the effective interaction of two actively contractile units is the opposite of the sign of the effective interaction of two passively contractile inclusions.[21,119,120] In both cases, the interactions depend on the distance between and relative orientations of the contractile units (which are often nonspherical in the biological systems). In both cases, the strength of the interaction is inversely proportional to the matrix rigidity and vanishes for infinitely rigid media. However, in the active case, the acto-myosin contractility stress itself is regulated by the cell and increases with substrate or matrix rigidity up to some saturation value; this can also be conceptualized by considering that the cell maintains a constant local strain - at least for soft substrates or matrices.[122] Experimentally, it is known that cell motility depends on substrate stiffness and cells can also attract or repel each other depending on substrate rigidity.[123] The elastic interactions can also lead to orientational order[17,116,119,124–126] (analogous to a nematic liquid crystal) or translational registry[18–20] (analogous to smectic order in liquid crystals) that depends on matrix stiffness in a nonmonotonic manner since the interaction strength decreases with rigidity, while the contractility magnitude, whose square also determines the net interaction magnitude, increases with rigidity.[21,122] This predicts a maximum for the order as a function of substrate rigidity, as observed in experiment, giving rise to an optimization of order by variation of the matrix rigidity.[17–20]

Before presenting the theoretical description of how acto-myosin contractility deforms the elastic surroundings in a long-range manner, thus leading to elastically mediated interactions of such "active inclusions," we briefly review the molecular basis[127] behind the coupling of cellular forces to the surrounding, passive elastic medium. Without such coupling, the medium would not be deformed and there would be no long-range mechanical interactions within or between cells. These connections occur at sites located on the cell periphery and are termed focal adhesions. They can be mesoscopic (e.g., micrometer) in size and consists of a long-lived (but locally dynamic on a molecular scale), complex, multicomponent,[128] protein assembly that connects the actin cytoskeleton to transmembrane adhesion receptors from the integrin family. These are then connected, on the extracellular side, to the substrate or extracellular matrix. (Small and transient adhesions are termed focal contacts.) A coarse-grained description of focal adhesions depicts a layered structure with the "bottom" layer coupled to the cell membrane and substrate (or extracellular matrix) and the "top" layer coupled to the actomyosin cytoskeleton. In the "lower" layer, the transmembrane adhesion receptors of the integrin family have large units that bind to the substrate and

© 2018 WILEY-VCH Verlag GmbH & Co. KGaA, Weinheim

smaller ones that bind to the cell. The cytoskeletal forces within the cell mechanically activate the integrins to conformations suitable to matrix binding.[129–132] The molecule[127] talin crosslinks adjacent integrin molecules over a distance of about 60 nm while also binding actin in the "upper" layer. Thus, talin, along with molecules such as vinculin and paxillin, are important components of the focal adhesion protein complex that couples the contractile cytoskeleton to the surrounding matrix. The focal adhesions also serve as signaling centers involved in regulating actin assembly and myosin activity by molecules from the Rho protein family. They also localize other molecules involved in cell motility and cell differentiation (such as focal adhesion kinase, FAK).

The displacement in the matrix at position $\vec{r}$ that is caused by a force dipole of magnitude p located at position $\vec{r}'$ is proportional to $p/|\vec{r}-\vec{r}'|^2$.[21] This has the same spatial dependence as the electrostatic potential in Coulomb's law for electrical dipoles except for the important difference due to the tensor nature of the force dipole that dictates a complex dependence of the matrix deformation on the relative orientations of the two force dipoles.[17,21,116,121] (We reiterate that the acto-myosin force dipoles we consider are not electrostatic or magnetic ones; only the terminology and scaling are similar.) The matrix elastic energy is a function of the relative orientation and distance between the dipoles. The resulting matrix forces affect the cellular adhesions, resulting in motion of the acto-myosin units or the cells themselves.

Two nearby dipoles each give rise to a strain field in the deformed matrix. The overlap of these two strains enters as part of the deformation energy of the matrix.[21,120,121] We denote this overlap or interaction energy by H, formed by the product of each force dipole moment and the strain field caused by its neighbor; the strain due to a given dipole is the spatial derivative of the displacement of the matrix caused by the contractility of that force dipole

$$H = \sum_{k\neq l} p_{ij}^{k} \varepsilon_{ij}^{l} \tag{20}$$

Here, p_{ij}^{k} and ε_{ij}^{l} are, respectively, the force dipole moment and the strain due to the kth and lth force dipoles, and i and j represent the x, y, and z directions. There is a mathematical similarity between this interaction and that of an electric dipole with an electric field. We wish to emphasize that the interaction of one dipole with the strain field of its neighbor is merely another way to express the elastic energy of the matrix or substrate. To obtain the force[18,121,133] exerted by the elastic medium on a cellular adhesion, we calculate the spatial derivative of the local elastic stress. This is proportional to the local strain for a linear elastic medium. For example, for two linear force dipoles oriented along the z-direction, the force in the z-direction applied to one dipole by the other is

$$F_z = -p_{zz}^{k} \frac{\partial \varepsilon_{zz}^{l}}{\partial z} \tag{21}$$

4.2. Experimental Examples of Contractility Induced Ordering

The previous section outlined the elements of the theory applying the force dipole concept to active, elastic systems such as acto-myosin filaments within the cellular cytoskeleton or entire contractile cells in gel-like matrices such as the extracellular matrix. While the cell is not in thermodynamic equilibrium (i.e., its internal structure does not conform to minimization of some free energy), the matrix is a passive material whose state is governed by free energy minimization. Thus, the surrounding elastic medium exerts forces on the cellular adhesions which will lead to a minimization of the matrix elastic energy.[108,121] These forces are then translated by the cell into motion or reorientation of its internal acto-myosin contractile units so that in mechanical equilibrium the net force on the contractile units and within the matrix is zero. Of course, neither the matrix nor the cells are governed entirely by the deterministic mechanical forces discussed till now and one must also include the effects of noise—both thermal and that arising from cellular biochemical activity. Assuming that these noise sources are correlated only on relatively short time scales compared to the experimental observations, one can approximate the probability of cellular orientational or translational order as being governed by a Boltzmann-like factor involving the energy H given by Equation (20) and an effective temperature that in the case of cells can be orders of magnitude larger than its thermal value.[18–21,112,124,134]

The net effect, is that the order or reorientation of the contractile units (or cells) induced by the matrix forces (due to the contractility of other units—or cells) is only partial, depending on the ratio of the interaction energy and the noise amplitude.[17,19,20] The most ordered configurations occur when the interaction energies are largest, which can be strongly dependent on the substrate or matrix rigidity as discussed above. For weaker interactions, the noise dominates and the contractile units (or cells) may be fairly disordered.

Experimental examples of these effects have been studied in the orientation of relatively short, acto-myosin fibers within stem cells plated from solution onto elastic substrates at time scales of 2–24 h.[17,135] A detailed analysis shows that the elastic interactions of the fibers (mediated by the intervening cytoskeleton and the substrate) tend to align them along the long axis of the cell, analogous to nematic ordering in liquid crystals. This effect is strongest at an optimal substrate rigidity since the contractility increases with rigidity (before saturating), while the elastic interactions tend to decrease with substrate rigidity. Indeed, the experiments clearly measure the existence of this optimal rigidity, at least for cells that are not too elongated. Highly elongated cells show an increase and then saturation of the orientational ordering of the acto-myosin fibers, perhaps due to steric hindrance or to a more subtle coupling of the initial shape of the cell and acto-myosin fiber growth. A similar effect of an optimal substrate elasticity is also observed when the cell aspect ratio is measured. Adding a drug that deactivates myosin contractility greatly suppresses the rigidity-dependent aspect ratio of these cells which become elongated as the acto-myosin fibers orient and increase in length.[136] This indicates the crucial role of active, myosin contractility in the orientational interactions.

The ordering of the relatively short, acto-myosin fibers in stem cells at early times may have important implications for the differentiation fate of these cells several days later. An

© 2018 WILEY-VCH Verlag GmbH & Co. KGaA, Weinheim

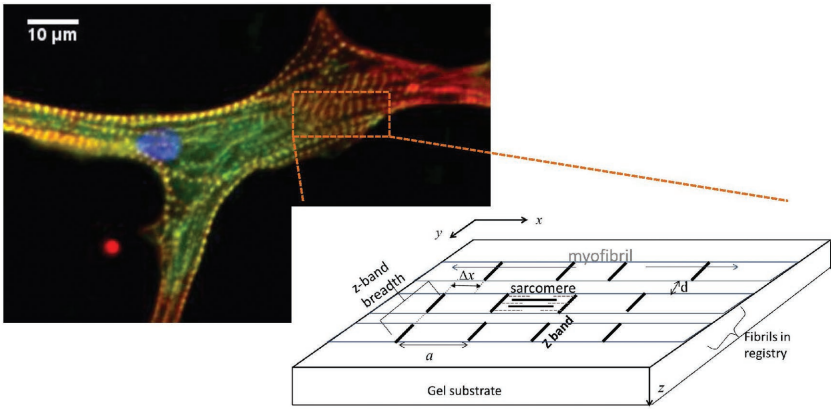

Figure 9. Chick cardiomyocyte cultured on collagen-I-coated 11 kPa polyacrylamide gel and stained for sarcomeric alpha actinin (green), filamentous actin (red), and DNA (blue) to visualize myofibril striations. The "blow-up" shows a schematic illustration of the experimental setup. Here, three aligned, parallel myofibrils are shown; the two fibrils indicated are in registry, whereas the third is off registry by a distance Δx. Each fibril is made of a repeating sarcomere unit (comprising alternating actin and myosin filaments, here shown by dashed and solid lines, respectively). The distance between neighboring z bands along a fibril, that is, the unit cell size or length of a sarcomere is denoted as a, whereas d is the transverse inter-fibril distance. Reproduced with permission.[19] Copyright 2015, Springer Nature.

earlier and striking experimental observation was that stem cells tended to differentiate into muscle cells in a relatively narrow range of substrate rigidity; on softer substrates (≈1 kPa) they differentiated into nerve or brain cells, while on stiffer substrates (≈50 kPa) they differentiated into bone cells.[8] This complex biological effect, involving signaling from the matrix that affects gene expression in the nucleus, may have its origins in the physics of acto-myosin fiber orientation that is maximized in the identical rigidity range where the differentiation fate was that of muscle cells.[17] Indeed, muscle cells are characterized by highly oriented and well-ordered acto-myosin fibers and the observation of orientational ordering at 2–24 h may indicate that the elastic interactions of the contractile units are an early-time cue that triggers differentiation into muscle. This suggests a crucial role for mechanics in regulating not only the structure of cells, but their function such as differentiation.

The elastic interactions of contractile, acto-myosin units can also explain observations of the registered organization (see **Figure 9**) of myosin in neighboring acto-myosin fibers in muscle cells such as cardiomyocytes.[18–20] This layering or stacking of myosins in fibers that can be separated by several hundred nm is analogous to smectic ordering in liquid crystals. The contractile forces due to one fiber with many contractile units along its length induce a spatially, periodically patterned strain field within the substrate with alternating regions of compression and expansion, which biases the positioning of the contractile units of a neighboring fibers.[105,133] By including the molecular noise inherent in cells, one can use the theory to map (see **Figure 10**) the measured, substrate rigidity dependence of registry onto that of the measured beating strains generated by cardiomyocytes. The good agreement of theory with experiments relates the correlated *beating* of heart cells to the *structural* registry of the myofibrils, which in turn is regulated by their elastic environment.[19,20] This is another example of how mechanical forces can affect both self-assembly and function in biological cells.

As mentioned, entire contractile cells can also be modeled in a coarse-grained manner as force dipoles that interact via the substrate or 3D matrix with nearby contractile cells.[21,107,110] A recent observation discussed in detail in the following section is that the beating dynamics of cardiomyocytes can be regulated by the beating of other nearby beating cells or even by an oscillating mechanical probe.[137,138] In contrast to the long-range, power-law decay of the substrate displacement as a function of distance from a force dipole, theory indicates that a dynamically beating dipole induces a substrate displacement that decays exponentially with distance from the source.[121] The decay length decreases as the product of the beating frequency and the substrate viscosity; as the frequency increases, the net displacement of the matrix away from the cell tends to zero.[121] Nevertheless, it has been observed and estimated theoretically that the elastic interactions of beating cells (or a beating cell and a mechanical probe) separated by up to about 100 μm are still sizable enough to affect the beating frequency.[138] Several regimes are observed and predicted as a function of the amplitude ratios and frequency differences, including complete entrainment of the cellular beating by the probe frequency and a regime (similar to structural discommensurations in spatially incommensurate lattices)[139] in which the beating is entrained for several periods and then stops before the cycle repeats itself.[121,138]

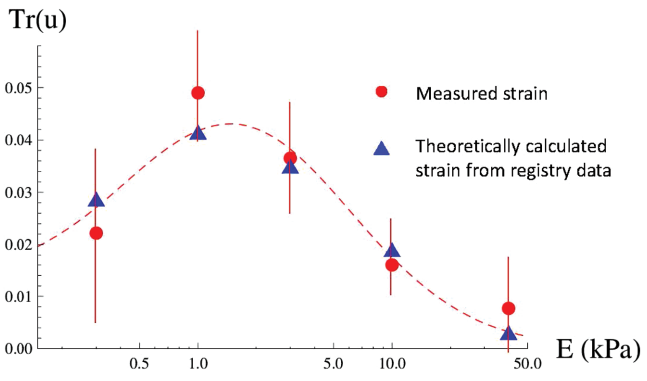

Figure 10. The z-band breadth data (zbb) are mapped to strain values using the theoretically derived expressions. The measured strain is shown as solid, red dots together with the experimental error bars. The dashed red line is an interpolated guide to the eye that joins the measured strain data points within their error bars. The blue triangles represent the strain values obtained by the theoretical mapping from the corresponding zbb measurements (for the same values of substrate elasticity) and show a close match with the experimentally measured strain values within the error bars. Reproduced with permission.[19] Copyright 2015, Springer Nature.

© 2018 WILEY-VCH Verlag GmbH & Co. KGaA, Weinheim

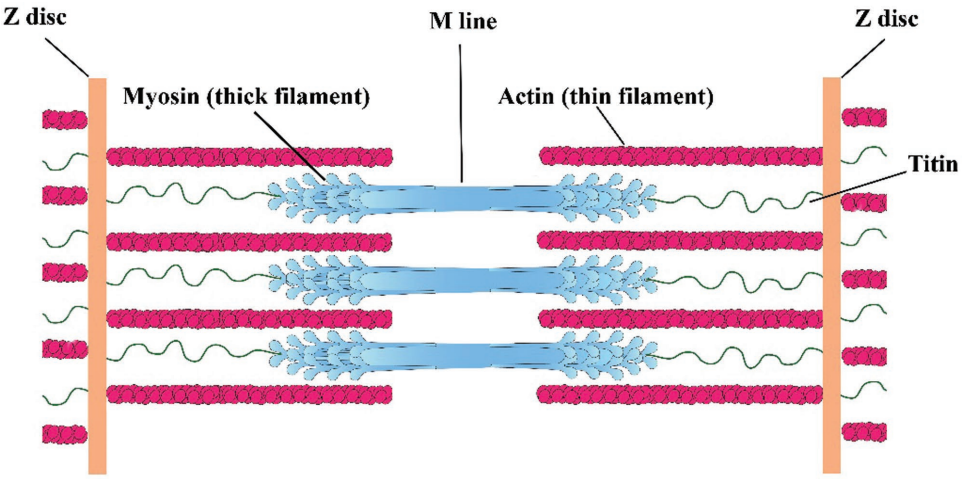

Figure 11. Schematic illustration of the sarcomere structure. The thick filaments of muscle consist of myosin motor molecules, assembled through interactions between their tails. During contraction, the globular heads of myosin bind the actin filaments (thin filaments) and pull them toward the center of the sarcomere. An elastic chain, comprising a series of immunoglobulin-like domains that can unfold as stress is applied, extends from the Z-disc to the M-line.

5. Active Mechanics and Modulation of Beating Cardiomyocytes

Cells are supported and connected in tissues by a viscoelastic background formed by an intricate, dynamic network of macromolecules termed the extracellular matrix. It provides physical scaffolding as well as crucial biochemical cues by regulating the availability of extracellular signaling molecules.[140] The biological cell can be thought of as a "living (active) rheometer," continuously probing the mechanical properties of its environment by exerting contractile forces on its surroundings, through the actomyosin machinery. The cellular contractile forces are transmitted to the ECM through cell–matrix adhesions (or cell–substrate in the case of 2D cultures), termed focal adhesions, and locally deform the matrix. Cells are able to sense the mechanical deformation field induced in their environment by either other cells or external mechanical loads. They respond to the nearby stresses or strains by adjusting their adhesions and cytoskeletal organization and by triggering biochemical transduction pathways that alter fundamental cellular processes.[8,17,141–148] The detailed molecular mechanisms underlying the conversion of mechanical cues into a biochemical signal are gradually being revealed.[132,143,149–155] Cell–ECM mechanical coupling is reciprocal. Cells continuously remodel the ECM and induce changes in its mechanics,[156–158] while environment mechanics regulate protein expression, secretion, and actomyosin contractility within the cells, thereby regulating cell elasticity, rigidity and contractility, and the mechanical forces that cells apply.[159]

The ability of cells to sense and respond to deformations they induce in their environment allows cells to communicate mechanically by detecting and responding to substrate strains generated by their neighbors. Some evidence has been accumulated over the past few years for the role of mechanical communication through the ECM in physiological processes and in synchronous behavior of interacting cells.[123,137,138,160,161]

We shall now focus on muscle cells and heart muscle cells (cardiomyocytes) in particular. In both skeletal and cardiac muscle, the cytoskeleton shows extremely well-ordered structures of repeated contractile units—called sarcomeres.[127] The sarcomere consists of an ordered array of parallel and partially overlapping thick and thin filaments. The thick filaments are assemblies of myosin motor proteins. The thin filaments composed of actin and associated proteins attached at their plus ends to a Z-disc at each end of the sarcomere[127] (see **Figure 11**). The myosin and actin filaments are packed together with almost crystalline regularity. In fact, this periodic structure is so highly organized that it shows a 3D diffraction pattern.[162–164] As shown in **Figure 12**, cardiac cells that are cultured on substrates with different rigidities differ in the number of sarcomeres, fiber alignment, and registry of neighboring sarcomeres.[19,20,165,166] The dependence of the sarcomeric cytoskeleton on substrate mechanics is an indication of the mechanical feedback between the cell and its substrate

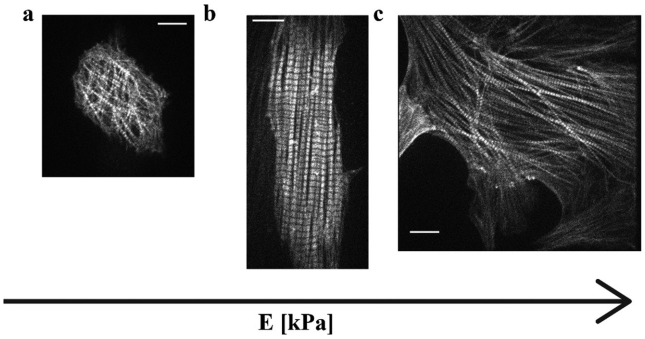

Figure 12. Representative images of cardiac cells on polyacrylamide substrates with varying Young's moduli. Actin is labeled using Lifeact-RFP: a) 1 kPa, b) 4 kPa, and c) 100 kPa. Cardiac cells are larger with increased rigidity and an optimal rigidity exists for optimal sarcomere alignment. Scale bar: 10 μm.

© 2018 WILEY-VCH Verlag GmbH & Co. KGaA, Weinheim

as mentioned above. We note that cell and ECM rigidities are orders of magnitude softer than atomic or molecular solids (kPa instead of MPa or GPa) due to the large distances between crosslinkers in these polymeric, water-swollen gels.[167] In cardiac physiology, sarcomeric cytoskeleton remodeling occur during development and under mechanical overload.[168,169] For example, an increase in mechanical load in the heart (e.g., high blood pressure) causes cardiac hypertrophy where the cardiac cells become larger due to sarcomere addition.

A spontaneously beating cardiac cell induces deformations in the underlying substrate that, for physiologically relevant rigidities (on the order of kPa), extend for several cell diameters and can be detected by neighboring beating cells (see **Figure 13**a,b).[121,137,138] The significance of mechanical communication between cardiac cells was explored by designing a mechanical device that consists of a tungsten probe that generates oscillatory deformations in the underlying substrate[137,138] (see Figure 13). Since there is no physical contact between the cell and the probe, the interaction is mediated solely by mechanical deformations of the elastic substrate. To construct a "mechanical cell," probe deformations were chosen in a way that mimic those generated by a neighboring beating cardiac cell.[138] Since the strain field generated by a beating cardiac cell is highly anisotropic (see Figure 13a,b), the direction and amplitude of probe-induced deformations were found to be of fundamental importance. After a "training period" of 10–15 min, the cardiac cell synchronizes its beating with that of the mechanical probe[138] (see Figure 13c). Cells can follow the probe oscillation frequency up to a certain threshold. At higher probe oscillation frequencies, cell dynamics turn into a bursting behavior involving fast and slow time scales (see Figure 13d). The fast frequency is dictated by the probe, while the slow frequency equals the spontaneous beating frequency of the cell prior to probe activation. Surprisingly, unlike pacing using electrical field stimulation, probe-induced beating rate was maintained by the cell for an hour after the stimulation was stopped, implying that long-term modifications induced by the mechanical stimulation occur within the cell (see Figure 13e).

Spontaneous beating of cardiac cells arises from self-sustained oscillations of the intracellular calcium concentration coupled to membrane depolarization–repolarization cycles.[170–172] Influx of Ca^{2+} ions into the cytoplasm, which result, for example, from membrane depolarization by an action potential, induces opening of Ryanodine receptors (RyRs) channels on an intracellular storage

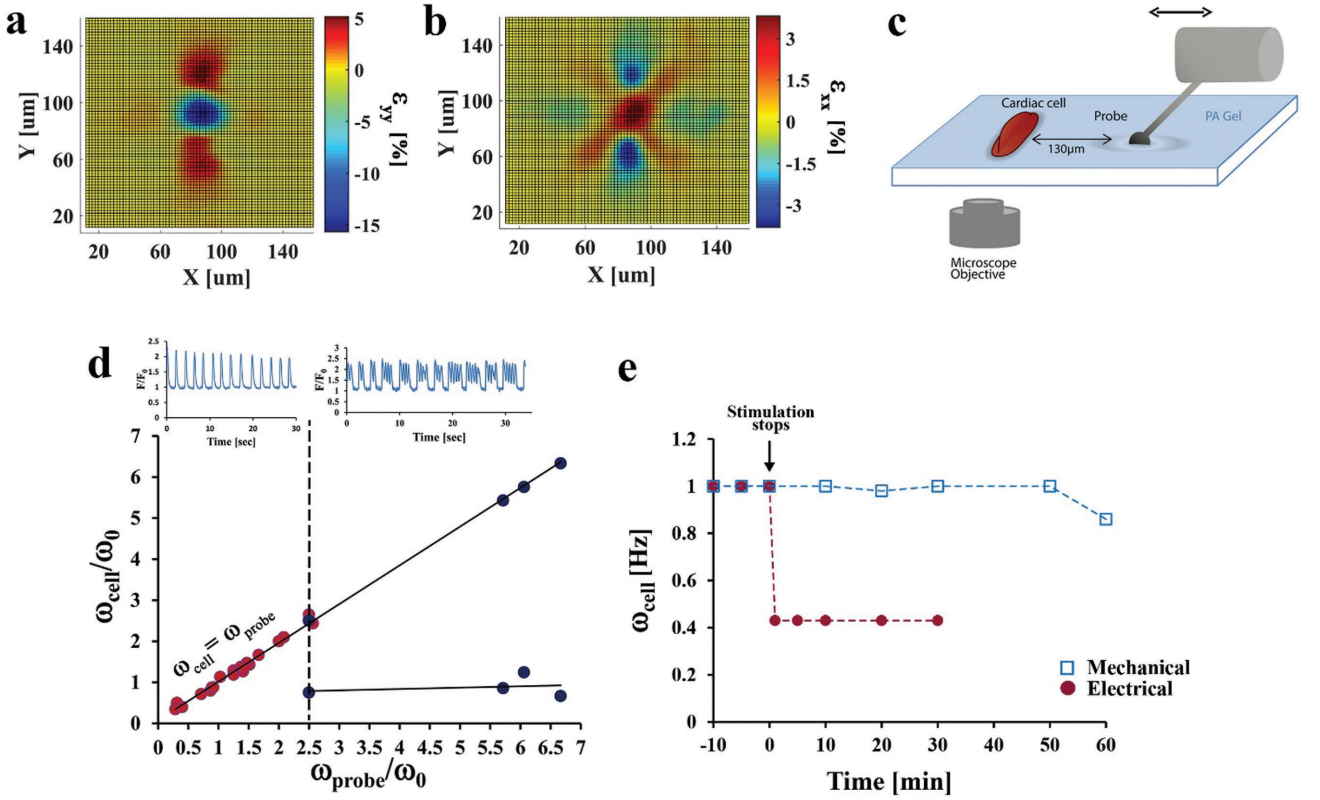

Figure 13. a,b) Strain field generated by a beating cardiac cell along the contraction axis (i.e., the direction of the long axis of the cell (a, *y*-axis)) and along the parallel direction (b, *x*-axis). c–e) Mechanical pacing of a spontaneously beating cardiac cell. c) Schematic representation of the experimental setup used for pacing neonatal rat cardiomyocytes using a mechanical probe. A tungsten probe applies an oscillatory stretch, thereby deforming the underlying substrate. d) Cell beating frequency after 10 min of mechanical stimulation (w_{cell}) as a function of probe frequency (w_{probe}) normalized by the spontaneous beating frequency of the cell before probe activation (w_0). Each point represents a single cell experiment. Above $w_{probe}/w_0 = 2.5$, cell dynamics turn into "bursting" behavior. e) Cell beating rate induced by mechanical stimulation persists over an hour after the mechanical stimulus stops, while the pacing performed by electrical field stimulation is transient. Representative behavior of a cell stimulated with a frequency of 1 Hz by a mechanical probe (empty blue squares) and by electrical field stimulation (filled red circles). In both cases, the spontaneous beating frequency of the cell before stimulation was $w_0 = 0.4$ Hz. c–e) Reproduced with permission.[138] Copyright 2016, Springer Nature.

© 2018 WILEY-VCH Verlag GmbH & Co. KGaA, Weinheim

named the sarcoplasmic reticulum (SR) in a process known as "Ca^{2+}-induced Ca^{2+} release." Elevation of intracellular calcium levels promotes binding of Ca^{2+} to TroponinC that in turn leads to a series of conformational rearrangements that reveal strong myosin binding sites on actin. This allows for myosin binding and acto-myosin contraction. Eventual decrease in calcium concentration, due to calcium pumps (e.g., sarcoendoplasmic reticulum calcium ATPase (SERCA)) and transporters (e.g., Na^+/Ca^{2+} exchanger) that transport Ca^{2+} out of the cytoplasm, leads to release of Ca^{2+} from Troponin C and process reversal.[170]

While mechanical signals are clearly able to remodel the sarcomeric cytoskeleton, the cytoskeleton was not remodeled in the time scale of the "mechanical cell" experiment.[138] Modifications to the biochemical machinery that governs spontaneous beating and electromechanical coupling in cardiac cells can account for the change in spontaneous beating frequency and electromechanical delay values. The mechanism that underlies mechanical communication in cardiac cell beating is still unclear and will require further study. In recent years, increased sensitivity of type 2 Ryanodine receptor (RyR2) channels through NADPH oxidase 2 (Nox2) activation in a microtuble-dependent manner has been shown to play a major role in mechanochemo transduction in the heart.[173,174]

It may well be that the level of remodeling involved depends on the time scale of the interaction. At short times, only the kinetics and sensitivity of ion channels, calcium pumps, and transporters is modified, while after a longer time cytoskeletal rearrangements occur. Therefore, cardiac cells behave as coupled "living" oscillators that are able to evolve as a result of mechanical coupling.

Spontaneous actomyosin oscillations occur in systems other than muscle cells. The collective motion of molecular motors can spontaneously generate periodic motion at all lengths scales, from the molecular level (as observed for the gliding motion of an optically trapped actin filament over a substrate densely coated with myosin motors[175]) through the cellular level (as observed in beating flagella or the contraction waves of a spreading fibroblast) to the tissue level (as observed during gastrulation in the developing embryo, where the tissue alternates between phases of actomyosin contractions and pauses where the constricted state of the cells is stabilized by cell–cell junction reorganization[176,177]). Cardiac cell beating is regulated by calcium oscillations; however, spontaneous oscillations with no regulatory chemical signal can occur in cases where the motors are acting against a resisting elastic force or in cases where two types of motors, moving in opposite directions, are involved.[176,178]

The dynamic coupling between cells and the ECM makes the cell–ECM a single, complex, and dynamically coupled unit. Cells were shown to locally remodel the ECM by, for example, aligning collagen fibers.[99,157,158] This remodeling leads to long-range, frequency-dependent mechanical interaction.[160,179] Mechanical coupling between cells is not limited to cardiac cells or oscillatory systems. Since all adherent cells apply traction forces (essential for cell adhesion and motility) on their environment, the latter gives rise to mechanical coupling between cells that can drive multi-cellular organization by directing cell migration and cellular orientation.[123,160,161]

Understanding the role of mechanical communication and the ability to manipulate it by modifying the mechanical properties of the environment, whether it is the natural extracellular matrix or an artificial scaffold, will pave the way for new strategies to biomaterial scaffold design that can support maturation and proper alignment of cardiomyocytes and promote synchronized cell beating.

6. Concluding Remarks

We have presented an introduction for materials scientists of the physical properties of active (energy-consuming) force generation in biological cells and contrasted this with the case of equilibrium (thermal) fluctuations that is familiar from materials and soft matter science. Examples that show novel behavior include red-blood-cell fluctuations, diffusion of beads in cells, and nonuniform active forces in egg cells (oocytes). We then focused on an in vitro system with active forces in which myosin molecular motors (activated by ATP) promote self-contraction and shape transformations in thin acto-myosin gels. The acto-myosin gels behave as poroelastic, active materials, as previously proposed for actin gels in living cells. These results may shed light on macroscopic shape changes of 2D tissues observed in various biological systems induced by myosin contractility, for example, gastrulation in developing embryos.

We next focused on nonmotile, adhered cells, where acto-myosin contractile forces within the cell are transmitted to the substrate or matrix via the adhesions that connect them. The stresses induced in the substrate act back on the cell and can order the acto-myosin segments either orientationally or translationally. This has been explored experimentally in stem cells and in the ordering of neighboring (but noncontacting) fibers in cardiomyocytes and in fibroblasts. The physical ordering has implications for biological function: in stem cells, the orientational ordering can anisotropically deform the nucleus, reorganize the chromatin (DNA) and impact differentiation, while in cardiomyocytes, the registered structure of neighboring fibers results in more coherent beating and higher cellular stress applied to its surroundings. In addition, the dependence of intra- and intercellular ordering on the rigidity of the surrounding matrix may inform tissue engineering applications. An experimental study of dynamical, mechanical signaling in beating heart cells (cardiomyocytes) was presented, as an example of oscillations of the acto-myosin network. The experiments demonstrate how an oscillating mechanical probe can "entrain" the frequency of cardiomyocyte beating. Furthermore, it was shown that the same mechanical effect can occur for two adjacent heart cells, separated by distances of several cell diameters. This may have important implications for synchronized beating and mechanical regulation of cardiac tissue that are of bioengineering and medical importance.

Acknowledgements

S.A.S. is grateful to the Israel-US Binational Science Foundation, the Israel Science Foundation, the Perlman Family Foundation, and a research grant from the Villalon family. A.B.-G. thanks the Israel Science Foundation (1618/15) for financial support. N.S.G. is the incumbent of the Lee and William Abramowitz Professorial Chair of Biophysics and this research was made possible in part by the generosity of the Harold Perlman family. N.S.G. acknowledges support from the ISF (Grant No. 580/12).

© 2018 WILEY-VCH Verlag GmbH & Co. KGaA, Weinheim

Conflict of Interest

The authors declare no conflict of interest.

Keywords

active matter, biological physics, cell mechanics, soft matter

Received: December 1, 2017
Revised: March 27, 2018
Published online:

[1] R. Phillips, J. Kondev, J. Theriot, H. G. Garcia, N. Orme, *Physical Biology of the Cell*, Garland Science, New York **2012**.
[2] S. A. Safran, *Statistical Thermodynamics of Surfaces, Interfaces, and Membranes*, Westview Press, Boulder, CO, USA **2003**.
[3] K. V. Iyer, S. Maharana, S. Gupta, A. Libchaber, T. Tlusty, G. V. Shivashankar, *PLoS One* **2012**, *7*, e46628.
[4] B. Chasan, J. Kondev, J. Theriot, H. Garcia, B. Chasan, *Am. J. Phys.* **2010**, *78*, 1230.
[5] A. B. Kolomeisky, M. E. Fisher, *Annu. Rev. Phys. Chem.* **2007**, *58*, 675.
[6] A. Vologodskii, *Phys. Life Rev.* **2006**, *3*, 119.
[7] D. Bracha, E. Karzbrun, G. Shemer, P. A. Pincus, R. H. Bar-Ziv, *Proc. Natl. Acad. Sci. USA* **2013**, *110*, 4534.
[8] A. J. Engler, S. Sen, H. L. Sweeney, D. E. Discher, *Cell* **2006**, *126*, 677.
[9] Y. Ideses, V. Erukhimovitch, R. Brand, D. Jourdain, J. S. Hernandez, U. R. Gabinet, S. A. Safran, K. Kruse, A. Bernheim-Groswasser, *Nat. Commun.* **2018**, *9*, 2461.
[10] J. Yoon, S. Cai, Z. Suo, R. C. Hayward, *Soft Matter* **2010**, *6*, 6004.
[11] W. Strychalski, R. D. Guy, *Biophys. J.* **2016**, *110*, 1168.
[12] E. Moeendarbary, L. Valon, M. Fritzsche, A. R. Harris, D. A. Moulding, A. J. Thrasher, E. Stride, L. Mahadevan, G. T. Charras, *Nat. Mater.* **2013**, *12*, 253.
[13] G. T. Charras, J. C. Yarrow, M. A. Horton, L. Mahadevan, T. J. Mitchison, *Nature* **2005**, *435*, 365.
[14] C. P. Heisenberg, Y. Bellaïche, *Cell* **2013**, *153*, 948.
[15] E. Hannezo, J. Prost, J.-F. Joanny, *Proc. Natl. Acad. Sci. USA* **2014**, *111*, 27.
[16] B. He, K. Doubrovinski, O. Polyakov, E. Wieschaus, *Nature* **2014**, *508*, 392.
[17] A. Zemel, F. Rehfeldt, A. E. X. Brown, D. E. Discher, S. A. Safran, *Nat. Phys.* **2010**, *6*, 468.
[18] B. M. Friedrich, A. Buxboim, D. E. Discher, S. A. Safran, *Biophys. J.* **2011**, *100*, 2706.
[19] K. Dasbiswas, S. Majkut, D. E. Discher, S. A. Safran, *Nat. Commun.* **2015**, *6*, 6085.
[20] MBInfo Web of Mechanobiology Institute, Singapore, https://www.mechanobio.info/cytoskeleton-dynamics/what-are-motor-proteins/what-steps-are-involved-in-the-myosin-powerstroke/ (accessed: July 2018).
[21] U. S. Schwarz, S. A. Safran, *Rev. Mod. Phys.* **2013**, *85*, 1327.
[22] T. Mura, *Micromechanics of Defects in Solids*, Springer, Dordrecht, The Netherlands **1987**.
[23] J. Howard, *Mechanics of Motor Proteins and the Cytoskeleton*, Oxford University Press, Oxford, UK **2001**.
[24] M. Murrell, P. W. Oakes, M. Lenz, M. L. Gardel, *Nat. Rev. Mol. Cell Biol.* **2015**, *16*, 48.
[25] C. P. Brangwynne, G. H. Koenderink, F. C. MacKintosh, D. A. Weitz, *Trends Cell Biol.* **2009**, *19*, 423.
[26] A. Caspi, R. Granek, E. Michael, *Phys. Rev. Lett.* **2000**, *85*, 5655.
[27] M. Drechsler, F. Giavazzi, R. Cerbino, I. M. Palacios, *Nat. Commun.* **2017**, *8*, 1520.
[28] D. Oriola, R. Alert, C. Jaume, *Phys. Rev. Lett.* **2017**, *118*, 088002.
[29] D. Humphrey, C. Duggan, D. Saha, D. Smith, J. Käs, *Nature* **2002**, *416*, 413.
[30] M. Almonacid, W. W. Ahmed, M. Bussonnier, P. Mailly, T. Betz, R. Voituriez, N. S. Gov, M.-H. H. Verlhac, *Nat. Cell Biol.* **2015**, *17*, 470.
[31] B. R. Parry, I. V Surovtsev, M. T. Cabeen, C. S. O. Hern, E. R. Dufresne, *Cell* **2014**, *156*, 183.
[32] A. Sonn-Segev, A. Bernheim-Groswasser, Y. Roichman, *J. Phys.: Condens. Matter* **2017**, *29*, 163002.
[33] A. Sonn-Segev, A. Bernheim-Groswasser, Y. Roichman, *Soft Matter* **2017**, *13*, 7352.
[34] G. H. Koenderink, Z. Dogic, F. Nakamura, P. M. Bendix, F. C. MacKintosh, J. H. Hartwig, T. P. Stossel, D. A. Weitz, *Proc. Natl. Acad. Sci. USA* **2009**, *106*, 15192.
[35] S. T. Spagnol, K. N. Dahl, *Integr. Biol.* **2014**, *6*, 523.
[36] S. Talwar, A. Kumar, M. Rao, G. I. Menon, G. V. Shivashankar, *Biophys. J.* **2013**, *104*, 553.
[37] C. R. Brown, C. Mao, E. Falkovskaia, M. S. Jurica, H. Boeger, *PLoS Biol.* **2013**, *11*, e1001621.
[38] N. Gov, A. G. Zilman, S. Safran, *Phys. Rev. Lett.* **2003**, *90*, 228101.
[39] D. Loi, S. Mossa, L. F. Cugliandolo, *Soft Matter* **2011**, *7*, 3726.
[40] D. Loi, S. Mossa, L. F. Cugliandolo, *Phys. Rev. E* **2008**, *77*, 051111.
[41] S. Wang, P. G. Wolynes, *J. Chem. Phys.* **2011**, *135*, 051101.
[42] E. Ben-Isaac, Y. Park, G. Popescu, F. L. H. Brown, N. S. Gov, Y. Shokef, *Phys. Rev. Lett.* **2011**, *106*, 1.
[43] N. Razin, R. Voituriez, J. Elgeti, N. S. Gov, *Phys. Rev. E* **2017**, *96*, 052409.
[44] J. Palacci, C. Cottin-Bizonne, C. Ybert, L. Bocquet, *Phys. Rev. Lett.* **2010**, *105*, 088304.
[45] H. Turlier, D. A. Fedosov, B. Audoly, T. Auth, N. S. Gov, C. Sykes, J. Joanny, G. Gompper, T. Betz, *Nat. Phys.* **2016**, *12*, 513.
[46] É. Fodor, M. Guo, N. S. Gov, P. Visco, D. A. Weitz, F. van Wijland, *EPL* **2015**, *110*, 48005.
[47] É. Fodor, W. W. Ahmed, M. Almonacid, M. Bussonnier, N. S. Gov, M.-H. Verlhac, T. Betz, P. Visco, F. van Wijland, *EPL* **2016**, *116*, 30008.
[48] D. Mizuno, C. Tardin, C. F. Schmidt, F. C. Mackintosh, *Science* **2007**, *315*, 370.
[49] J. Gladrow, N. Fakhri, F. C. MacKintosh, C. F. Schmidt, C. P. Broedersz, *Phys. Rev. Lett.* **2016**, *116*, 248301.
[50] C. Battle, C. P. Broedersz, N. Fakhri, V. F. Geyer, J. Howard, C. F. Schmidt, F. C. MacKintosh, *Science* **2016**, *352*, 604.
[51] F. S. Gnesotto, F. Mura, J. Gladrow, C. P. Broedersz, *Rep. Prog. Phys.* **2018**, *81*, 066601.
[52] É. Fodor, C. Nardini, M. E. Cates, J. Tailleur, P. Visco, F. van Wijland, *Phys. Rev. Lett.* **2016**, *117*, 038103.
[53] C. Nardini, É. Fodor, E. Tjhung, F. van Wijland, J. Tailleur, M. E. Cates, *Phys. Rev. X* **2017**, *7*, 0210.
[54] A. Kaiser, S. Babel, B. Ten Hagen, C. Von Ferber, H. Löwen, *J. Chem. Phys.* **2015**, *142*, 124905.
[55] A. Ghosh, N. S. Gov, *Biophys. J.* **2014**, *107*, 1065.
[56] C. A. Weber, R. Suzuki, V. Schaller, I. S. Aranson, A. R. Bausch, E. Frey, *Proc. Natl. Acad. Sci. USA* **2015**, *112*, 10703.
[57] J. B. Manneville, P. Bassereau, D. Lévy, J. Prost, *Phys Rev Lett* **1999**, *82*, 4356.
[58] P. Girard, J. Prost, P. Bassereau, *Phys. Rev. Lett.* **2005**, *94*, 88102.
[59] M. D. E. A. Faris, D. Lacoste, J. Pécréaux, J.-F. Joanny, J. Prost, P. Bassereau, *Phys. Rev. Lett.* **2009**, *102*, 38102.
[60] N. Gov, *Phys. Rev. Lett.* **2004**, *93*, 268104.
[61] R. Granek, S. Pierrat, *Phys. Rev. Lett.* **1999**, *83*, 872.
[62] R. Rodríguez-García, I. López-Montero, M. Mell, G. Egea, N. S. Gov, F. Monroy, *Biophys. J.* **2015**, *108*, 2794.

© 2018 WILEY-VCH Verlag GmbH & Co. KGaA, Weinheim

[63] P. Almendro-Vedia, V. G. Natale, M. Mell, S. Bonneau, F. Monroy, F. Joubert, I. López-Montero, *Proc. Natl. Acad. Sci. USA* **2017**, 201701207.
[64] F. Brochard, J. F. Lennon, *J. Phys.* **1975**, *36*, 1035.
[65] S. Levin, R. Korenstein, *Biophys. J.* **1991**, *60*, 733.
[66] Y. K. Park, C. A. Best, K. Badizadegan, R. R. Dasari, M. S. Feld, T. Kuriabova, M. L. Henle, A. J. Levine, G. Popescu, *Proc. Natl. Acad. Sci. USA* **2010**, *107*, 6731.
[67] Y. Park, C. A. Best, T. Auth, N. S. Gov, S. A. Safran, G. Popescu, S. Suresh, M. S. Feld, *Proc. Natl. Acad. Sci. USA* **2010**, *107*, 1289.
[68] L. C.-L. Lin, N. Gov, F. L. Brown, *J. Chem. Phys.* **2006**, *124*, 074903.
[69] N. S. Gov, S. A. Safran, *Biophys. J.* **2005**, *88*, 1859.
[70] M. Guo, A. J. Ehrlicher, M. H. Jensen, M. Renz, J. R. Moore, R. D. Goldman, J. Lippincott-Schwartz, F. C. Mackintosh, D. A. Weitz, *Cell* **2014**, *158*, 822.
[71] E. Ben-Isaac, E. Fodor, P. Visco, F. Van Wijland, N. S. Gov, *Phys. Rev. E: Stat., Nonlinear, Soft Matter Phys.* **2015**, *92*, 1.
[72] T. Toyota, D. A. Head, C. F. Schmidt, D. Mizuno, *Soft Matter* **2011**, *7*, 3234.
[73] P. Bohec, F. Gallet, C. Maes, S. Safaverdi, P. Visco, F. van Wijland, *Eur. Lett.* **2013**, *102*, 50005.
[74] P. Bursac, B. Fabry, X. Trepat, G. Lenormand, J. P. Butler, N. Wang, J. J. Fredberg, S. S. An, *Biochem. Biophys. Res. Commun.* **2007**, *355*, 324.
[75] É. Fodor, K. Kanazawa, H. Hayakawa, P. Visco, F. van Wijland, *Phys. Rev. E* **2014**, *90*, 42724.
[76] É. Fodor, V. Mehandia, J. Comelles, R. Thiagarajan, N. S. Gov, P. Visco, F. van Wijland, D. Riveline, *Biophy. J.* **2018**, *114*, 939.
[77] C. O. Reichhardt, C. Reichhardt, *Ann. Rev. Condens. Matter Phys.* **2017**, *8*, 51.
[78] L. Angelani, A. Costanzo, R. D. Leonardo, *EPL* **2011**, *96*, 68002.
[79] M. B. Wan, C. J. R. Olson, Z. Nussinov, C. Reichhardt, *Phys. Rev. Lett.* **2008**, *101*, 018102.
[80] M. O. Magnasco, *Phys. Rev. Lett.* **1993**, *71*, 1477.
[81] J. Tailleur, M. E. Cates, *EPL* **2009**, *86*, 60002.
[82] N. Razin, R. Voituriez, J. Elgeti, N. S. Gov, *Phys. Rev. E* **2017**, *96*, 032606.
[83] A. P. Liu, D. A. Fletcher, *Nat. Rev. Mol. Cell Biol.* **2009**, *10*, 644.
[84] O. Siton-Mendelson, A. Bernheim-Groswasser, *Cell Adhes. Migr.* **2016**, *10*, 461.
[85] B. Li, Y.-P. Cao, X.-Q. Feng, H. Gao, *Soft Matter* **2012**, *8*, 5728.
[86] J. A. Gemmer, S. C. Venkataramani, *Nonlinearity* **2012**, *25*, 3553.
[87] B. Audoly, A. Boudaoud, *Phys. Rev. Lett.* **2003**, *91*, 086105.
[88] A. E. Shyer, T. Tallinen, N. L. Nerurkar, Z. Wei, E. S. Gil, D. L. Kaplan, C. J. Tabin, L. Mahadevan, *Science* **2013**, *342*, 212.
[89] J. Dervaux, M. Ben Amar, *Phys. Rev. Lett.* **2008**, *101*, 068101.
[90] U. Nath, B. C. W. Crawford, R. Carpenter, E. Coen, *Science* **2003**, *299*, 1404.
[91] H. Liang, L. Mahadevan, *Proc. Natl. Acad. Sci. USA* **2011**, *108*, 5516.
[92] A. Livshits, L. Shani-Zerbib, Y. Maroudas-Sacks, E. Braun, K. Keren, *Cell Rep.* **2017**, *18*, 1410.
[93] Y. Klein, E. Efrati, E. Sharon, *Science* **2007**, *315*, 1116.
[94] F. Backouche, L. Haviv, D. Groswasser, A. Bernheim-Groswasser, *Phys. Biol.* **2006**, *3*, 264.
[95] Y. Ideses, A. Sonn-Segev, Y. Roichman, A. Bernheim-Groswasser, *Soft Matter* **2013**, *9*, 7127.
[96] J. Alvarado, M. Sheinman, A. Sharma, F. C. MacKintosh, G. H. Koenderink, *Nat. Phys.* **2013**, *9*, 591.
[97] M. P. Murrell, M. L. Gardel, *Proc. Natl. Acad. Sci. USA* **2012**, *109*, 20820.
[98] M. Lenz, T. Thoresen, M. L. Gardel, A. R. Dinner, *Phys. Rev. Lett.* **2012**, *108*, 238107.
[99] X. Xu, S. A. Safran, *Phys. Rev. E* **2015**, *92*, 1.
[100] X. Xu, S. A. Safran, *Phys. Rev. E* **2017**, *95*, 052415.
[101] M. Schuppler, F. C. Keber, M. Kröger, A. R. Bausch, *Nat. Commun.* **2016**, *7*, 13120.
[102] B. Guo, W. H. Guilford, *Proc. Natl. Acad. Sci. USA* **2006**, *103*, 9844.
[103] K. Keren, P. T. Yam, A. Kinkhabwala, A. Mogilner, J. A. Theriot, *Nat. Cell Biol.* **2009**, *11*, 1219.
[104] A. Mogilner, A. Manhart, *Annu. Rev. Fluid Mech.* **2018**, *50*, 347.
[105] K. Dasbiswas, S. Hu, F. Schnorrer, S. A. Safran, A. D. Bershadsky, *Philos. Trans. R. Soc., B* **2018**, *373*, 1747.
[106] P. W. Oakes, E. Wagner, C. A. Brand, D. Probst, M. Linke, U. S. Schwarz, M. Glotzer, M. L. Gardel, *Nat. Commun.* **2017**, *8*, 15817.
[107] P. W. Oakes, S. Banerjee, M. C. Marchetti, M. L. Gardel, *Biophys. J.* **2014**, *107*, 825.
[108] D. Ben-Yaakov, R. Golkov, Y. Shokef, S. A. Safran, *Soft Matter* **2015**, *11*, 1412.
[109] H. Wagner, H. Horner, *Adv. Phys.* **2006**, *23*, 587.
[110] K. Dasbiswas, E. Alster, S. A. Safran, *Sci. Rep.* **2016**, *6*, 27692.
[111] R. De, A. Zemel, S. A. Safran, *Nat. Phys.* **2007**, *3*, 655.
[112] U. Faust, N. Hampe, W. Rubner, N. Kirchgesner, S. Safran, B. Hoffmann, R. Merkel, N. Kirchgessner, S. Safran, B. Hoffmann, R. Merkel, *PLoS One* **2011**, *6*, e28963.
[113] M. Guo, A. F. Pegoraro, A. Mao, E. H. Zhou, P. R. Arany, Y. Han, D. T. Burnette, M. H. Jensen, K. E. Kasza, J. R. Moore, F. C. Mackintosh, J. J. Fredberg, D. J. Mooney, J. Lippincott-Schwartz, D. A. Weitz, *Proc. Natl. Acad. Sci. USA* **2017**, *c*, 201705179.
[114] A. Zemel, R. De, S. A. Safran, *Curr. Opin. Solid State Mater. Sci.* **2011**, *15*, 169.
[115] D. H. Boal, *Mechanics of the Cell*, Cambridge University Press, Cambridge **2012**.
[116] A. Zemel, I. B. Bischofs, S. A. Safran, *Phys. Rev. Lett.* **2006**, *97*, 1.
[117] U. S. Schwarz, S. A. Safran, *Phys. Rev. Lett.* **2002**, *88*, 048102.
[118] H. Wagner, H. Horner, *Adv. Phys.* **1974**, *23*, 587.
[119] I. B. Bischofs, U. S. Schwarz, *Proc. Natl. Acad. Sci. USA* **2003**, *100*, 9274.
[120] I. B. Bischofs, S. A. Safran, U. S. Schwarz, *Phys. Rev. E: Stat., Nonlinear, Soft Matter Phys.* **2004**, *69*, 1.
[121] O. Cohen, S. A. Safran, *Soft Matter* **2016**, *12*, 6088.
[122] M. Ghibaudo, A. Saez, L. Trichet, A. Xayaphoummine, J. Browaeys, P. Silberzan, A. Buguin, B. Ladoux, *Soft Matter* **2008**, *4*, 1836.
[123] C. A. Reinhart-King, M. Dembo, D. A. Hammer, *Biophys. J.* **2008**, *95*, 6044.
[124] B. M. Friedrich, S. a. Safran, *Soft Matter* **2012**, *8*, 3223.
[125] B. Gilboa, D. Gillo, O. Farago, A. Bernheim-Groswasser, *Soft Matter* **2009**, *5*, 2223.
[126] D. Gillo, B. Gilboa, R. Gurka, A. Bernheim-Groswasser, *Phys. Biol.* **2009**, *6*, 036003.
[127] B. Alberts, A. Johnson, J. Lewis, M. Raff, K. Roberts, P. Walter, *Molecular Biology of the Cell*, Garland Science, New York **2008**.
[128] S. E. Winograd-Katz, R. Fässler, B. Geiger, K. R. Legate, *Nat. Rev. Mol. Cell Biol.* **2014**, *15*, 273.
[129] E. Puklin-Faucher, M. P. Sheetz, *J. Cell Sci.* **2009**, *122*, 179.
[130] J. Li, T. A. Springer, *Proc. Natl. Acad. Sci. USA* **2017**, *114*, 4685.
[131] A. Nicolas, B. Geiger, S. A. Safran, *Proc. Natl. Acad. Sci. USA* **2004**, *101*, 12520.
[132] D. Riveline, E. Zamir, N. Q. Balaban, U. S. Schwarz, T. Ishizaki, S. Narumiya, Z. Kam, B. Geiger, A. D. Bershadsky, *J. Cell Biol.* **2001**, *153*, 1175.
[133] S. Hu, K. Dasbiswas, Z. Guo, Y.-H. Tee, V. Thiagarajan, P. Hersen, T.-L. Chew, S. A. Safran, R. Zaidel-Bar, A. D. Bershadsky, *Nat. Cell Biol.* **2017**, *19*, 133.
[134] S. A. Safran, R. De, *Phys. Rev. E: Stat., Nonlinear, Soft Matter Phys.* **2009**, *80*, 4.
[135] A. Zemel, F. Rehfeldt, A. E. Brown, D. E. Discher, S. A. Safran, *J. Phys.: Condens. Matter* **2010**, *22*, 194110.
[136] F. Rehfeldt, A. E. X. Brown, M. Raab, S. Cai, A. L. Zajac, A. Zemel, D. E. Discher, *Integr. Biol.* **2012**, *4*, 422.

© 2018 WILEY-VCH Verlag GmbH & Co. KGaA, Weinheim

[137] X. Tang, P. Bajaj, R. Bashir, T. A. Saif, *Soft Matter* **2011**, *7*, 6151.
[138] I. Nitsan, S. Drori, Y. E. Lewis, S. Cohen, S. Tzlil, *Nat. Phys.* **2016**, *12*, 472.
[139] F. C. Frank, J. H. van der Merwe, *Proc. R. Soc. London, Ser. A* **1949**, *198*, 205.
[140] T. Rozario, D. W. DeSimone, *Dev. Biol.* **2010**, *341*, 126.
[141] A. D. Bershadsky, N. Q. Balaban, B. Geiger, *Annu. Rev. Cell Dev. Biol.* **2003**, *19*, 677.
[142] F. Chowdhury, S. Na, D. Li, Y. C. Poh, T. S. Tanaka, F. Wang, N. Wang, *Nat. Mater.* **2010**, *9*, 82.
[143] B. Geiger, J. P. Spatz, A. D. Bershadsky, *Nat. Rev. Mol. Cell Biol.* **2009**, *10*, 21.
[144] C. M. Lo, H. B. Wang, M. Dembo, Y. L. Wang, *Biophys. J.* **2000**, *79*, 144.
[145] J. Y. Wong, A. Velasco, P. Rajagopalan, Q. Pham, *Langmuir* **2003**, *19*, 1908.
[146] A. J. Engler, C. Carag-Krieger, C. P. Johnson, M. Raab, H.-Y. Tang, D. W. Speicher, J. W. Sanger, J. M. Sanger, D. E. Discher, *J. Cell Sci.* **2008**, *121*, 3794.
[147] A. K. Harris, P. Wild, D. Stopak, *Science* **1980**, *208*, 177.
[148] R. J. Pelham, Y. l. Wang, *Mol. Biol. Cell* **1999**, *10*, 935.
[149] V. Vogel, *Annu. Rev. Biophys. Biomol. Struct.* **2006**, *35*, 459.
[150] V. Vogel, M. Sheetz, *Nat. Rev. Mol. Cell Biol.* **2006**, *7*, 265.
[151] T. Luo, K. Mohan, P. A. Iglesias, D. N. Robinson, *Nat. Mater.* **2013**, *12*, 1064.
[152] C. Ellison, Y. V. Brun, *Curr. Biol.* **2015**, *25*, R113.
[153] P. a. Janmey, R. T. Miller, *J. Cell Sci.* **2011**, *124*, 9.
[154] N. Q. Balaban, U. S. Schwarz, D. Riveline, P. Goichberg, G. Tzur, I. Sabanay, D. Mahalu, S. Safran, A. Bershadsky, L. Addadi, B. Geiger, *Nat. Cell Biol.* **2001**, *3*, 466.
[155] N. Wang, J. D. Tytell, D. E. Ingber, *Nat. Rev. Mol. Cell Biol.* **2009**, *10*, 75.
[156] X. Ma, M. E. Schickel, M. D. Stevenson, A. L. Sarang-Sieminski, K. J. Gooch, S. N. Ghadiali, R. T. Hart, *Biophys. J.* **2013**, *104*, 1410.
[157] M. S. Hall, F. Alisafaei, E. Ban, X. Feng, C.-Y. Hui, V. B. Shenoy, M. Wu, *Proc. Natl. Acad. Sci. USA* **2016**, *113*, 14043.
[158] J. Notbohm, A. Lesman, P. Rosakis, D. A. Tirrell, G. Ravichandran, *J. R. Soc., Interface* **2015**, *12*, 20150320.
[159] J. D. Humphrey, E. R. Dufresne, M. A. Schwartz, *Nat. Rev. Mol. Cell Biol.* **2014**, *15*, 802.
[160] J. P. Winer, S. Oake, P. A. Janmey, *PLoS One* **2009**, *4*, e6382.
[161] T. E. Angelini, E. Hannezo, X. Trepat, J. J. Fredberg, D. A. Weitz, *Phys. Rev. Lett.* **2010**, *104*, 168104.
[162] K. P. Roos, A. F. Leung, *Biophys. J.* **1987**, *52*, 329.
[163] G. H. Pollack, T. Iwazumi, H. E. ter Keurs, E. F. Shibata, *Nature* **1977**, *268*, 757.
[164] D. R. Cleworth, K. A. Edman, *J. Physiol.* **1972**, *227*, 1.
[165] S. Majkut, T. Idema, J. Swift, C. Krieger, A. Liu, D. E. Discher, *Curr. Biol.* **2013**, *23*, 2434.
[166] A. J. Engler, C. Carag-Krieger, C. P. Johnson, M. Raab, H. Y. Tang, D. W. Speicher, J. W. Sanger, J. M. Sanger, D. E. Discher, *J. Cell Sci.* **2008**, *121*, 3794.
[167] M. Rubinstein, R. Colby, *Polymer Physics*, Oxford University Press, Oxford, UK **2003**.
[168] B. Russell, M. W. Curtis, Y. E. Koshman, A. M. Samarel, *J. Mol. Cell. Cardiol.* **2010**, *48*, 817.
[169] H. Yang, L. P. Schmidt, Z. Wang, X. Yang, Y. Shao, T. K. Borg, R. Markwald, R. Runyan, B. Z. Gao, *Sci Rep.* **2016**, *6*, 20674.
[170] D. M. Bers, *Nature* **2002**, *415*, 198.
[171] T. A. Quinn, P. Kohl, *Prog. Biophys. Mol. Biol.* **2012**, *110*, 257.
[172] E. G. Lakatta, V. A. Maltsev, T. M. Vinogradova, *Circ. Res.* **2010**, *106*, 659.
[173] B. L. Prosser, C. W. Ward, W. J. Lederer, *Science* **2011**, *333*, 1440.
[174] Z. Jian, H. Han, T. Zhang, J. Puglisi, L. T. Izu, J. A. Shaw, E. Onofiok, J. R. Erickson, Y.-J. Chen, B. Horvath, R. Shimkunas, W. Xiao, Y. Li, T. Pan, J. Chan, T. Banyasz, J. C. Tardiff, N. Chiamvimonvat, D. M. Bers, K. S. Lam, Y. Chen-Izu, *Sci. Signaling* **2014**, *7*, ra27.
[175] P.-Y. Plaçais, M. Balland, T. Guérin, J.-F. Joanny, P. Martin, *Phys. Rev. Lett.* **2009**, *103*, 158102.
[176] K. Kruse, D. Riveline, *Curr. Top. Dev. Biol.* **2011**, *95*, 67.
[177] A. C. Martin, M. Kaschube, E. F. Wieschaus, *Nature* **2009**, *457*, 495.
[178] F. Jülicher, *C. R. Acad. Sci., Ser. IV: Phys., Astrophys.* **2001**, *2*, 849.
[179] Q. Shi, R. P. Ghosh, H. Engelke, C. H. Rycroft, L. Cassereau, J. A. Sethian, V. M. Weaver, J. T. Liphardt, *Proc. Natl. Acad. Sci. USA* **2014**, *111*, 658.

© 2018 WILEY-VCH Verlag GmbH & Co. KGaA, Weinheim